HYDROGRAPHY AND BOTTOM BOUNDARY LAYER DYNAMICS: INFLUENCE ON INNER SHELF SEDIMENT MOBILITY, LONG BAY, NC

Luke A. Davis

A Thesis Submitted to the
University of North Carolina Wilmington in Partial Fulfillment
Of the Requirements for the Degree of
Master of Science

Department of Geography and Geology

University of North Carolina Wilmington

2006

Approved by

Advisory Committee

_____ _____

_____ _____
Chair

Accepted by

_____
Dean, Graduate School

This thesis has been prepared in a style and format
consistent with
Estuarine, Coastal and Shelf Science.

TABLE OF CONTENTS

ABSTRACT

Storm-driven processes produced by atmospheric and meteorological forcing dictate sediment transport events in the bottom boundary layer on the inner continental shelf. This study examined the hydrography and bottom boundary layer dynamics of two typical storm events affecting coastal North Carolina, a hurricane and the November event consisting of two small consecutive extratropical storms during the autumn of 2005. Two upward-looking 1200-kHz Acoustic Doppler Current Profilers (ADCP) were deployed at two separate locations on the inner continental shelf of northern Long Bay, North Carolina at water depths of less than 15 m. Both instruments profiled the overlying water column in 0.35 m bins beginning at a height of 1.35 m above the bottom (mab). Simultaneous measurements of wind speed and direction, wave and current parameters, and acoustic backscatter were coupled with output from a bottom boundary layer (bbl) model to describe the hydrography and boundary layer conditions during each event. The bbl model also was used to generate current and suspended sediment concentration profiles and to quantify sediment transport in the boundary layer during each storm. Both study sites exhibited similar temporal trends in response to changing physical forcing mechanisms, but wave heights during the November event were higher than waves associated with the hurricane. Both near-bottom mean and subtidal currents, however, were of greater magnitude during the hurricane. Suspended sediment transport during the November event exceeded transport associated with the hurricane by 25-70%. Substantial spatial variations in sediment transport existed throughout both events. For both storms, along-shelf sediment transport exceeded across-shelf transport and was closely associated with the magnitudes and directions of the subtidal currents. Given the substantial variations in sediment type across the bay, complex shoreline configuration, and local bathymetry, the sediment transport rates reported here are very

site specific. However, the general hydrography associated with the two storms is representative of conditions across northern Long Bay.

ACKNOWLEDGEMENTS

I would first like to thank Dr. Lynn Leonard who encouraged and guided me with unending support and enthusiasm throughout this project. I would also like to thank the remainder of my faculty committee, Dr. Gregg Snedden, Dr. Michael Benedetti, and Dr. Fred Bingham whose advice led to the successful completion of this manuscript.

I would like to acknowledge Ken Hathaway and the U.S. Army Corps of Engineers for allowing the ADCP data to be available for me during this project. Dr. Gregg Snedden and Dr. Ansley Wren were both key in assisting me with MATLAB and implementing the bottom boundary layer model used in this research. I would also like to thank CORMP technicians Jay Souza, Dave Wells, and Steve Hall, who were essential in diving operations and general data collection. Further thanks go to the captains and crew of the *R/V Cape Fear* and *R/V Seahawk*.

This research was funded by the National Oceanic & Atmospheric Administration, Award # NA16RP2675 to the Coastal Ocean Research and Monitoring Program at UNCW. I would also like to thank the UNCW Graduate School, the College of Arts and Sciences, and the Department of Geography and Geology for their financial support of my graduate research and academic studies.

DEDICATION

I would like to dedicate this thesis to the geology faculty in the Department of Geology and Geography at Georgia Southern University from 2000-2004. These individuals encouraged me to pursue research in a variety of disciplines within the geological sciences as an undergraduate and are responsible for many of my early academic accomplishments.

LIST OF TABLES

LIST OF FIGURES

INTRODUCTION

Sediment transport events on inner shelf margins are driven largely by increased wave orbital velocities coupled with sustained wind-driven currents associated with meteorological forcing (Williams and Rose, 2001; Kim et al., 1997; Madsen et al., 1993; Xu and Wright, 1993). Describing these synoptic conditions is difficult, but the emergence of coastal observing systems has provided meteorological and oceanographic data at sufficient temporal and spatial scales to describe air-sea interactions storm events. Further, when used in conjunction with direct measures of turbidity and sea floor characteristics before, during, and after storm passage, the physical data can be used to describe and quantify sediment mobilization processes associated with specific storm events.

Coastal North Carolina is frequently affected by two types of storms, extratropical systems and hurricanes (Dolan et al., 1988). Extratropical systems, also referred to as midlatitude wave cyclones and nor'easters, are low-pressure circulations that recur with varying intensities every 3 to 12 days between October and April with maximum storm frequency between December and March. According to Dolan et al. (1988), approximately 30-35 storms affect the region annually with 80% occurring from October-April. Most of these storms are low magnitude, short duration events, though some, such as the "Halloween Storm" in October 1991 produce large waves and high winds for several days along the Atlantic Coast (Dolan and Davis, 1992; Wright et al., 1994). Hurricanes usually develop in the tropical Atlantic between June 1 and November 30 and periodically impact the North Carolina coast with peak frequency occurring in August through October. Over the last decade, nine hurricanes and four tropical storms made

landfall or tracked through the region. The frequency of category 2 and 3 hurricanes was higher in the 1990's compared to previous decades. This increase in coastal storm frequency in recent years has increased public and managerial interest in processes leading to beach erosion and in processes controlling the distribution of offshore sand that is suitable for beach renourishment projects. Similarly, because storm conditions mobilize sediments on the seabed, understanding the impact of sediment movement on hardbottom habitat viability and fisheries is also of interest to resource managers in the region. These topics are vital to the economy and ecology of coastal North Carolina and require a better understanding of how the coastal ocean responds physically to storm passage which would allow for the development of more successful management strategies.

Previous studies have recorded near-bottom fluid flows and sediment mobility during fair weather and storm conditions (Wright et al., 1991; Cacchione et al., 1994; Wright et al., 1994; Pepper and Stone, 2002). These studies have concluded that inner shelf processes are dominated by storm-driven currents and may provide the primary mechanism to move sediment in the across-shelf direction (Trowbridge and Young, 1989; Wright et al., 1991). Additional studies (e.g. Cacchione et al., 1994; Wren and Leonard, 2005) suggested that wave and current bottom stresses initiate sediment mobilization on the inner shelf and provide the mechanism that determines sediment availability for transport.

In Onslow Bay, North Carolina (Fig. 1), several regional studies have shown that wave-current interactions and storm swell are the primary mechanisms leading to significant sediment resuspension on the middle and inner continental shelf (Wren, 2004;

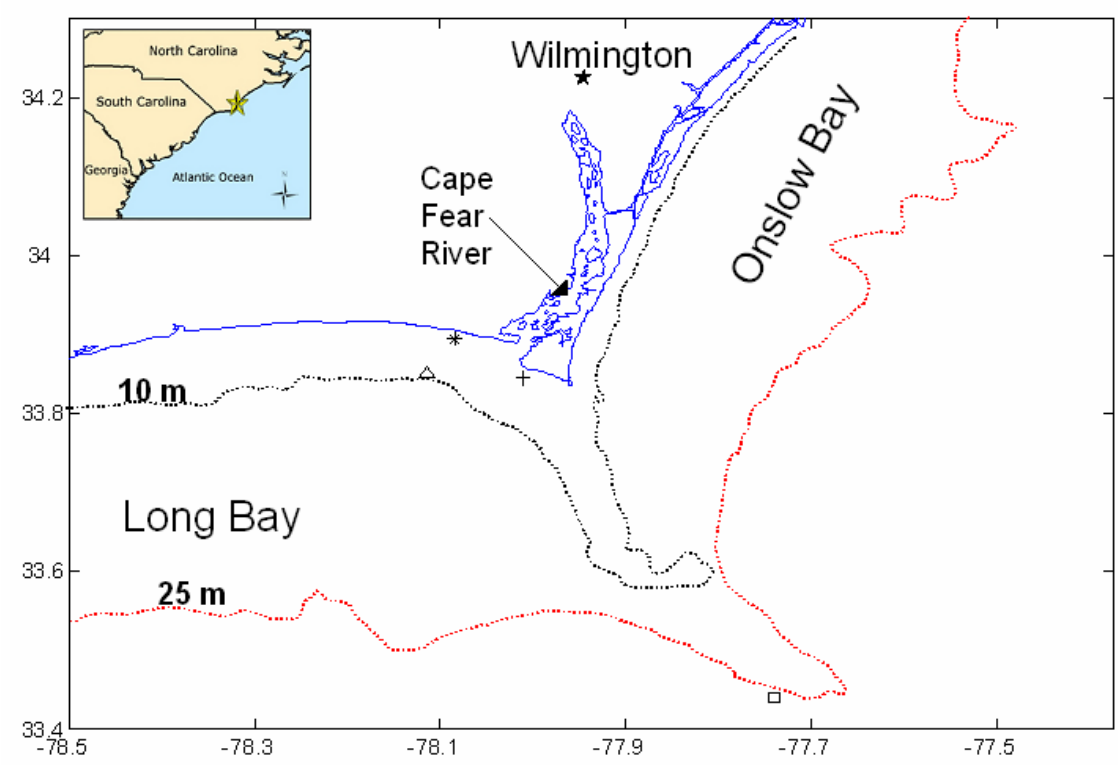

Fig. 1. The study area and surrounding offshore waters. The bay is bordered to the northeast by Cape Fear and Frying Pan Shoals. The Cape Fear River provides freshwater input to the upper bay. Instrumentation is designated with the following symbols: △ = LB1M; * = LB2M; + = LB3M; □ = NDBC buoy 41013.

Marshall 2004). Wren and Leonard (2005) found that while increased wave orbital velocities associated with storm swell provide the primary mechanism for suspending material from the seabed, subtidal currents provide the mechanism responsible for transport of the suspended material along or across the mid-continental shelf. Marshall (2004) observed that although increased wave orbital velocity on the inner shelf seabed during storms may cause appreciable sediment resuspension only subtle changes in sediment texture occurred. Both of these studies largely focused on the effects of Hurricane Isabel in 2003. Dolan et al. (1988) concluded that extratropical storms might be more significant in terms of overall sediment movement on the inner continental shelf because they occur with greater frequency. This observation is consistent with Wright et al. (1994) who suggested that extratropical storms, regardless of their magnitude, are critical to sediment transport on many time scales due to their recurrence interval.

A paucity of oceanographic data exists with respect to the effect of storms on sediment mobility in northern Long Bay, NC. This area lies within the North Carolina coastal corridor that is frequently affected by tropical and extratropical storms, but is buffered from the full impact of some of these systems due to the presence of an east-west trending coastline along its northern boundary (Fig. 1). The primary goal of this study is to identify and describe the physical mechanisms and bottom boundary layer dynamics during two coastal storms that mobilized sediment on the sediment-starved inner shelf of northern Long Bay, NC. Specifically, the objectives are: (1) to compare the spatial and temporal variability of the hydrography and sediment response in Long Bay during autumn 2005 and (2) to apply a bottom boundary layer model to quantify nearshore conditions and sediment mobility associated with the passage of Hurricane

Ophelia and the November event, a period consisting of the passage of two small extratropical storms with associated frontal systems.

STUDY AREA

Long Bay is located off the southeastern coast of North Carolina (Fig. 1). It occupies the southernmost section of the Carolina Cape complex that comprises the northern region of the South Atlantic Bight (SAB; Pietrafesa, et al., 1985). The bay is bounded by Cape Fear and Frying Pan Shoals to the northeast, Cape Romain to the southwest, and the shelf edge and Gulf Stream to the east. The shelf width at the 50 m isobath is approximately 80 km off Cape Fear and increases to 110 km in the central sections of the bay. The study area for this project is located on the inner shelf of northern Long Bay. This section of the inner shelf is adjacent to the mouth of the Cape Fear River and is characterized by water depths of less than 15 m. The primary forcing mechanisms recognized to influence the inner shelf (0-20m) are tides, winds, and river inflow (Atkinson and Menzel, 1985). In the study area, the mean tidal range is 1.3 m and was dominated by the M_2 constituent (NOAA, 2006). Mean annual significant wave heights is 0.6 m and with a dominant period of 6.5 s as measured from an upward-looking 1200 k-Hz Acoustic Doppler Current Profiler (ADCP) at LB1M. Wind direction was variable throughout the year but tended to blow toward the east-southeast from January until May, northward throughout the summer, and southwestward for the remainder of the year. The shifts in wind direction are associated with shifts in the Azores-Bermuda High and the weaker Ohio Valley High anticyclonic systems (Blanton et al., 1985). These general wind patterns are periodically interrupted by the passage of coastal storms

including extratropical cyclones and tropical storms. During this study, wind patterns associated with coastal storms rotated as a storm tracked over the region.

The inner shelf in the study area receives outflow from the Cape Fear River (CFR). The CFR is a relatively low discharge river system with a mean annual discharge of 275 $m^3 s^{-1}$ (1969-2005) and high annual variability (standard deviation $\approx$ 300 $m^3 s^{-1}$). The mainstem of the CFR originates in the Piedmont physiographic province of North Carolina at the convergence of the Haw and Deep Rivers, approximately 35 km southwest of Raleigh, NC. Two major tributaries, the Northeast Cape Fear River and the Black River converge with the CFR just north of Wilmington. Unlike the mainstem CFR, which drains brownwater systems of the Piedmont and upper Coastal Plain, these tributaries are primarily blackwater Coastal Plain rivers that drain vast floodplains and swamps (Mallin, 2006). These low-gradient rivers contain a high amount of dissolved organic acids, but low concentrations of suspended solids. Total suspended solids (TSS) in the blackwater tributaries are usually <10 mg l^{-1}, whereas TSS concentrations in the brownwater tributaries range from 5-35 mg l^{-1} (Renfro et al., 2004). Overall, the lower CFR has relatively low TSS concentrations due to the influence from its blackwater tributaries (Mallin, 2006).

Despite its proximity to the Cape Fear River, northern Long Bay is considered sediment-starved. The inner shelf near the mouth of the CFR in northern Long Bay is characterized by a thin veneer of sediment types ranging from muddy fine sand to shell hash. The majority of the sediment near the CFR mouth is composed of poorly sorted sand, but grades into fine sand and silt in the distal sections (McLeod and Cleary, 2000). Battisto and Friedrichs (2002) also observed predominantly medium to very fine sands in

this region. For this study, surface sediment grab samples were collected to validate sediment characteristics existing at each of the study sites. The mean grain size was highly variable and consisted of coarse sand ($\overline{x}$ = 0.065 cm) at LB2M and fine sand ($\overline{x}$ = 0.017 cm; Fig. 2) at LB3M. Previously, Slattery (2004) observed that the grain size of bottom sediments in the vicinity of LB2M also exhibited temporal variability; presumably due to river inputs and/or reworking of underlying material. To assess the vertical variations in grain size at LB2M, divers collected two 30 cm boxcores adjacent to LB2M. Both cores exhibited a 5-10 cm layer of coarse sand mean overlying fine sand (Fig. 3).

The thin veneer of surface sediment throughout the northern section of the bay overlies, from west to east, the Cretaceous Pee Dee Formation, the Paleocene Beaufort Formation, the Eocene Castle Hayne Formation, and the Oligocene River Bend Formation (Hoffman, et al. 1999; Fig. 4). Of these formations, the Castle Hayne and River Bend Formations are the exposed units within the study area. According to Figure 4, the two sites, LB2M and LB3M, are located in the Castle Hayne and River Bend Formations, respectively. These Formations consist of bryozoan biomicrudite and molluscan biosparrudite with thin units of dolomitic muddy quartz sand, which crop out in the study area and host a variety of hardbottom habitats. Bioerosion of these outcrops provides little sediment to the high-energy inner shelf (Hoffman, et al. 1999).

METHODS AND INSTRUMENTATION

River discharge from the Cape Fear River was collected from the CORMP website (www.cormp.org) which is calculated using and algorithm determined by Carpenter and Yonts (1979). Hourly wind data were collected from NDBC buoy 41013

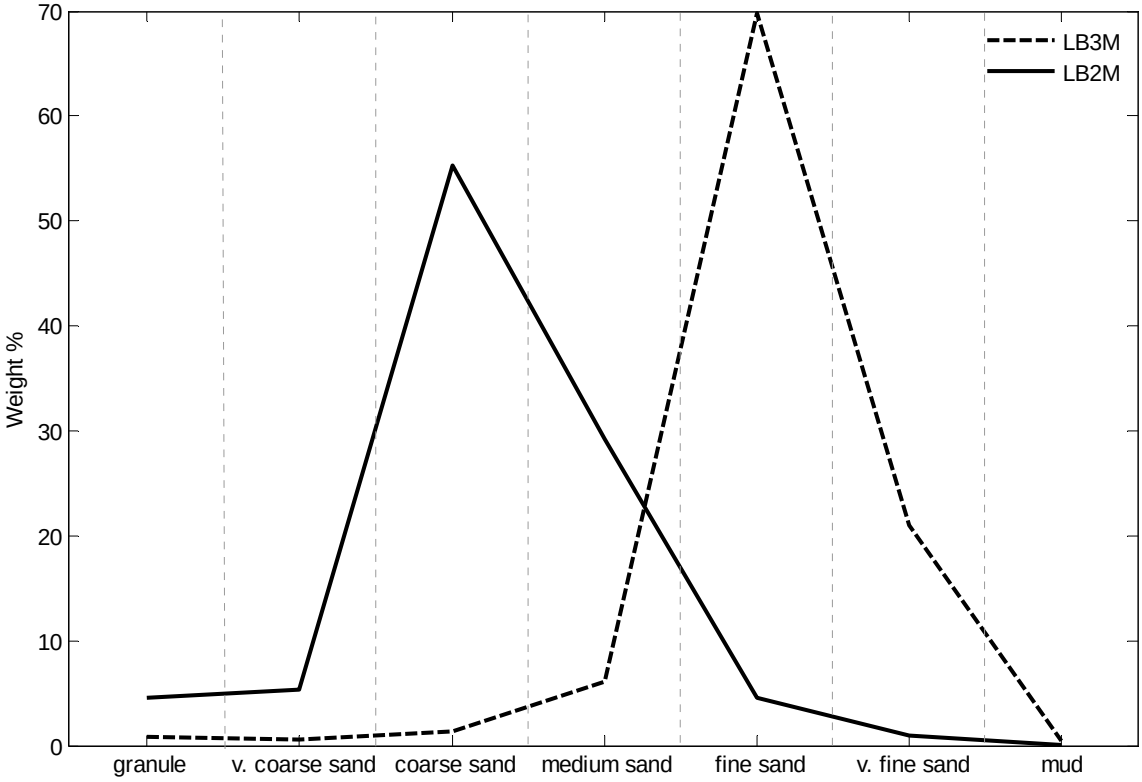

Fig. 2. Frequency distribution curves for sediments in the study area. The mean grain size for LB2M is coarse sand and fine sand for LB3M. The weight percent and the midpoint of each grain type were used to create the bottom boundary layer (bblm) profiles.

Fig. 3. Boxcore collected at LB2M on July 27, 2006. Coarse sand overlies fine sand in the shallow cores taken at this site.

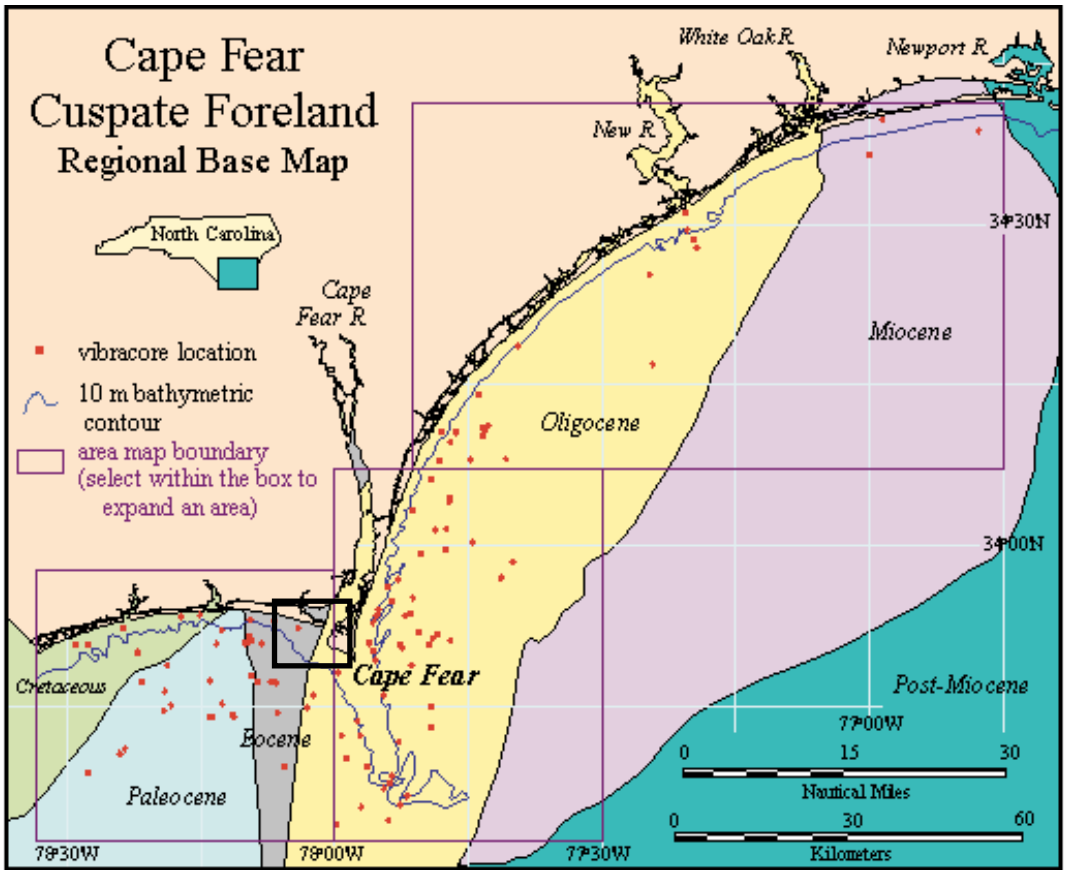

Fig. 4. A generalized geologic map of Onslow and Long Bays, North Carolina (adapted from Hoffman et al, 1999). The study area is designated with a black box near Cape Fear. The Castle Hayne and River Bend Formations crop out in the study area.

located on Frying Pan Shoals at the northern boundary of Long Bay approximately 60 km southeast of the study area (Fig. 1). Wave and current data were collected with two upward-looking 1200-kHz RDI Workhorse Sentinel ADCP's. The first site, LB2M, was located 1.8 km offshore of Oak Island and 40 km southwest of Wilmington at a depth of 7 m. The second site, LB3M, was located 0.9 km offshore of Bald Head Island at a depth of 5.8 m and approximately 5.7 km east of LB2M (Fig. 1). Both instruments profiled the overlying water column in 0.35 m bins beginning at a height of 1.35 m above bottom (mab). Measurements were collected at a rate of 0.5 Hz over a 6-minute sampling burst. One burst was collected every 10 minutes. Wave data were recorded every 4 hours at LB2M and every 3 hours at LB3M. For all mean and subtidal current data, the along-shelf axis was taken at 15º south of east for LB2M and 22º south of east for LB3M. Positive along-shelf was eastward towards Cape Fear and positive across-shelf was towards the coast. To measure relative changes in turbidity, the beam-averaged echo amplitude from the ADCP was used. This technique is useful for approximating relative changes in suspended particulate matter in the water column, overlying sandy substrates (Traykovski et al., 1999; Battisto, 2000; Williams and Rose, 2001). Using a methodology outlined by RD Instruments, a more accurate estimation of the absolute backscatter in units of decibels was calculated (Deines, 1999). A Lanczos cosine filter with a half-amplitude cutoff period of 40 hours was applied to all current and ABS data to minimize the tidal variability. Measurements of pre- and post-storm sediment thickness above the bedrock were collected along permanent 30-m transect lines in 5 m increments deployed east and north of the LB1M. Transects were not established at the

other two sites. The grain-size distributions of the seafloor sediments were determined by sieving using a modified Folk (1980) method.

A bottom boundary layer (bbl) model (Styles and Glenn, 2002) was used to calculate bed shear stress and critical shear velocities due to currents and the combined effects of wave-current interaction at the seabed based on the median grain size. From these calculations, the bbl model also calculated current velocity as well as suspended sediment concentration and transport profiles from 1.35 mab to the seabed using the sum of the weight percents for seven different grain sizes derived from bottom sediment grab samples (Fig.2; Wren and Leonard, 2005). The currents used in the profiles are burst-averaged over a 10-minute sampling burst. This bbl model used in this study evolved from over 25 years of shelf circulation modeling associated with nonlinear wave-current interactions in the boundary layer (Grant and Madsen, 1979; Glenn and Grant, 1987; Styles and Glenn, 2000, 2002).

Input data used in the model included: (1) mean near-bottom currents U_r measured at a 1.35 mab reference elevation (Z_r), (2) near-bottom orbital velocities U_b and excursion amplitudes A_b, and (3) wave and current incidence angle Φ_{cw}. These input parameters were determined from ADCP data in MATLAB prior to the implementation of the bbl model. Bottom r.m.s. orbital velocities, U_b, were calculated using equation 1.1:

$$U_b = \frac{\sqrt{2}\omega a}{\sinh\left(\frac{2\pi d}{L}\right)} \qquad \text{Eq. 1.1}$$

where U_b = wave orbital velocity in cm s^{-1}, ω= angular frequency, $a = \frac{H_{rms}}{2}$ in m, d= water depth in m, and L = wavelength in m.

The bbl model also calculates the critical shear stress threshold based on skin friction and the critical Shield's parameter. The critical shear velocity is the velocity necessary to initiate movement of the median grain size and is calculated using equation 1.2:

$$U_{*crit} = \sqrt{\frac{\tau_{crit}}{\rho}} \qquad \text{Eq. 1.2}$$

where U_{*crit} = critical shear velocity in cm s^{-1}, τ_{crit} = critical shear stress in N m^{-2}, and ρ = density of seawater (1.025 kg m^{-3}). It should be noted here that this study does not differentiate between bed load and suspended load. According to Wright et al. (1991), the critical shear velocity necessary to suspend the median grain size would exceed the U_{*crit} value calculated for this study.

RESULTS

Autumn 2005 Hydrography

Regional Forcing Mechanisms

During autumn 2005, the mean discharge of the Cape Fear River was 80 m^3 s^{-1}, about 40% of the 2005 annual mean of 196 m^3 s^{-1}. With the exception of subsequent runoff from the occasional tropical system, discharge in southeastern U.S. rivers is usually low in summer and early autumn due to high rates of evapotranspiration (Hupp, 2000). The period of lowest discharge occurred prior to Hurricane Ophelia on 8 September (28.4 m^3 s^{-1}; Fig. 5a).

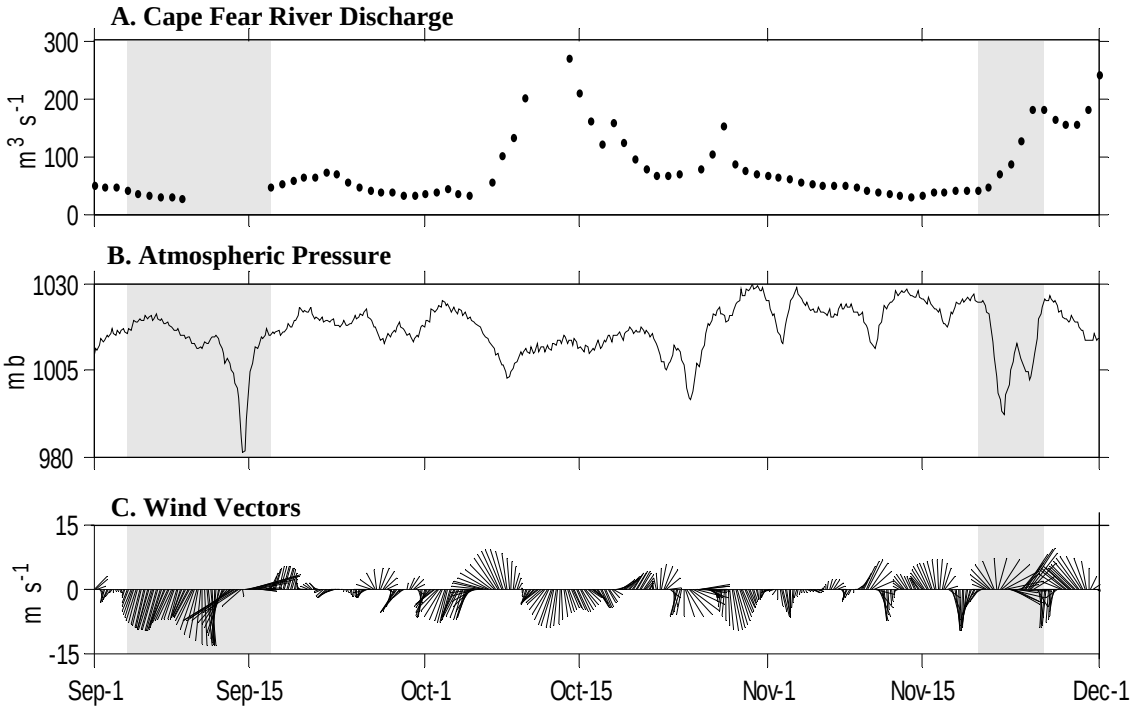

Fig. 5. Regional forcing mechanisms in Autumn 2005. (**a.**) Mean daily discharge of the Cape Fear River; (**b.**) Atmospheric pressure collected from NDBC Buoy 41013; (**c.**) 40-hr lowpassed wind velocity vectors. In 5c, a line extending upward from the x-axis indicates winds blowing toward shore and a line extending to the right indicates wind blowing east toward Cape Fear. Hurricane Ophelia and the November event are identified with shadeboxes.

Wind direction during the deployment period was variable, but southward and southwestward winds occurred for almost half of the study period. The strengthening of the Ohio Valley High influenced the autumn wind direction, which produced southwestward wind stress over the study area (Blanton et al., 1985). Winds exceeded 8 m s^{-1} for 4% of the deployment and these velocities were associated with the passage of Hurricane Ophelia and several extratropical systems in late October and late November. Over the study duration, winds did not exceed 10 m s^{-1} except during Hurricane Ophelia. During this event, maximum sustained easterly winds of 14.3 m s^{-1} were observed on 14 September 2005 (Fig 5c). Excluding Hurricane Ophelia, the maximum wind velocities (9.3 m s^{-1}) was associated with the November event. Because these two events were the strongest systems in terms of wind velocity impacting the study area during the study period, they will be used to quantify sediment mobility and to assess spatial variations in sediment mobility later in this paper.

A harmonic analysis of near-bottom currents in the bottom boundary layer using T_TIDE in MATLAB indicated that the lunar semi-diurnal M_2 tidal constituent dominated the tidal currents during the study period (Pawlowicz et al., 2002). This result was consistent with previous studies showing that the M_2 accounted for 80% of the tidal energy in Onslow Bay (Pietrafesa et al., 1985). The M_2 was highly elliptical and oriented shore parallel at both sites, but the magnitudes differed. The major axis of the tidal ellipse at LB3M was approximately 5 times greater than the axis at LB2M (Fig. 6).

Water Column and Sediment Response

The subtidal currents were predominantly eastward at LB2M and onshore at LB3M. During wind events the current flow was dominated by along-shelf flow (Fig.

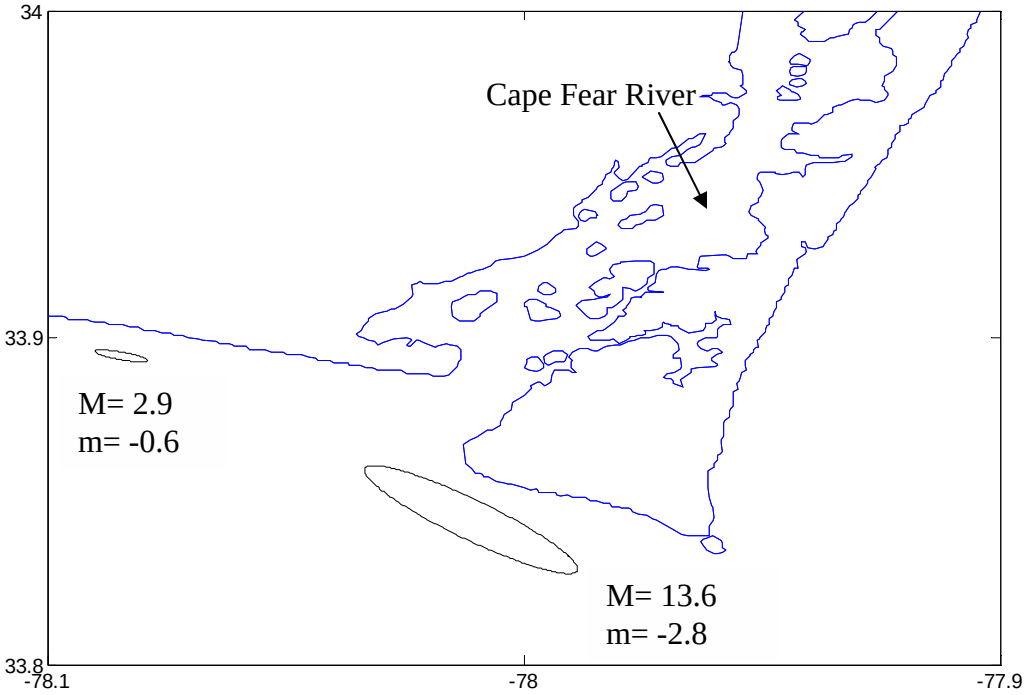

Fig. 6. M_2 tidal ellipses for LB2M (left) and LB3M (right). M is the major axis component, and m = minor axis component in cm s^{-1}. Ellipses are represented at identical scales to illustrate M_2 tidal variations between the two sites.

7b,c). The subtidal current velocity at LB3M was approximately 40% higher than the magnitude of the subtidal current at LB2M for most of the deployment (Fig. 7b, c). The across-shelf component was usually positive (onshore) at both sites whereas the along-shelf component varied in direction between the two sites. At LB2M, the net flow was positive (eastward), wheras at LB3M, the net flow was slightly negative (westward). While LB3M periodically experienced sustained currents in the across-shelf direction, subtidal currents at LB2M were almost exclusively along-shelf. Table 1 summarizes the net subtidal along-/across-shelf directional components during autumn 2005.

Maximum near-bottom subtidal currents were usually coincident with wind events. This pattern was particularly evident at LB3M where strong onshore currents were commonly associated with sustained offshore winds. The difference in wind and current direction at LB3M was most likely due to upwelling as bottom currents moved onshore to maintain the continuity of the ocean surface as winds forced water offshore. This pattern was not evident at LB2M where current magnitude was typically smaller and the current showed a consistent along-shelf component. The maximum subtidal current at both sites occurred late on 14 September and were 16.8 cm s^{-1} at 1800 UTC at LB2M and 38.6 cm s^{-1} at LB3M. These strong currents were the result of sustained along-shelf winds from Hurricane Ophelia 13-16 September. The rotating wind fields associated with Hurricane Ophelia and the November event increased the along-shelf subtidal currents at both sites with a more profound change at LB3M. The November event, with weaker winds and shorter duration than Ophelia, resulted in a more subdued shift in the along-shelf subtidal currents from their respective fair weather directions.

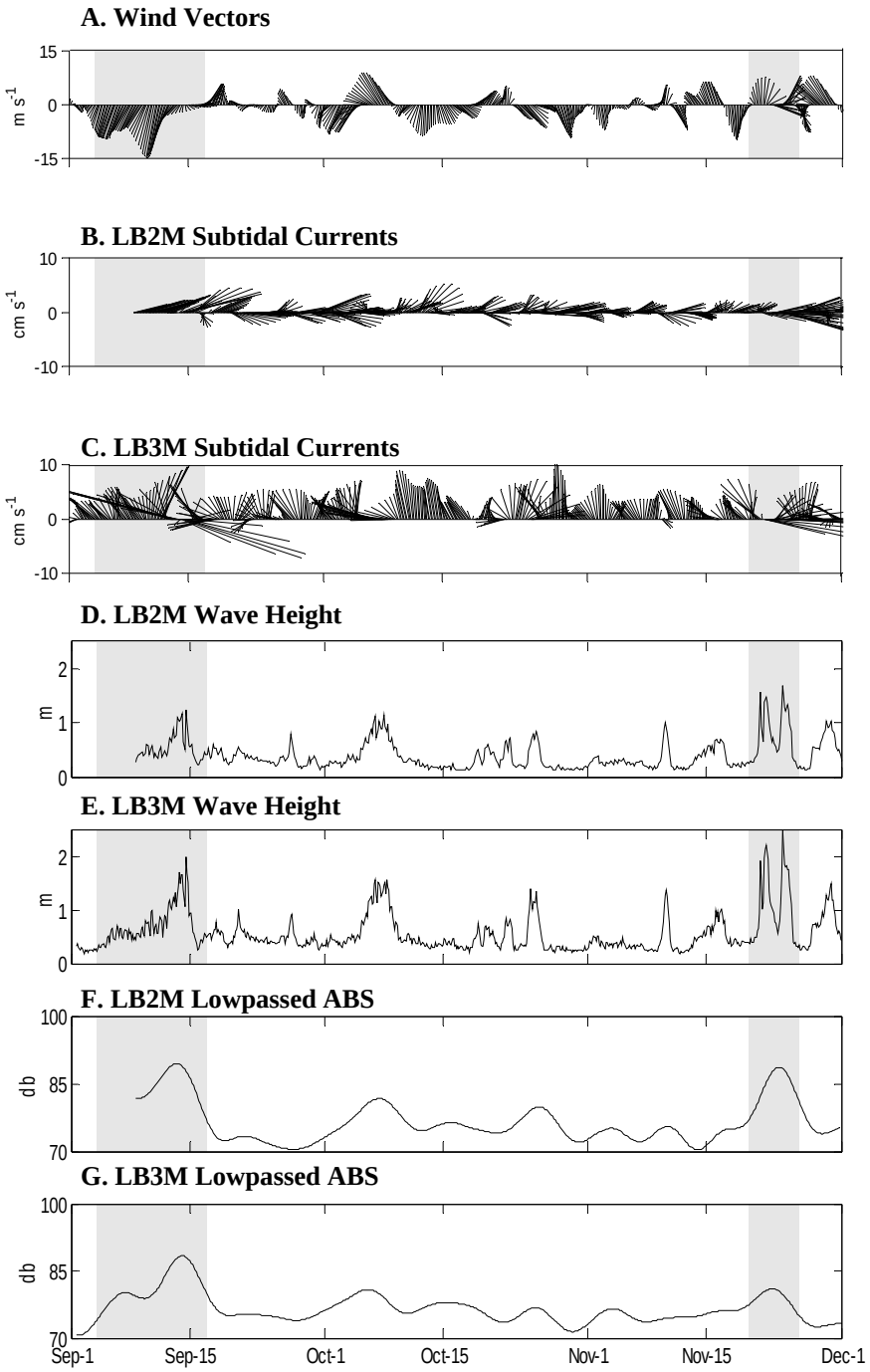

Fig. 7. Autumn 2005 hydrography and acoustic backscatter signal (ABS); (**a.**) Lowpassed wind vectors; (**b.**) LB2M subtidal currents; (**c.**) LB3M subtidal currents; (**d.**) LB2M wave height; (**e.**) LB3M wave height; (**f.**) LB2M lowpassed ABS; (**g.**) LB3M lowpassed ABS. On panels a-c, the same convention as Fig. 5c is used. All vectors point in the direction they are moving toward. Instrument failure occurred at LB2M from 1-8 September.

Table 1. Summary of the along-/across-shelf current magnitudes (cm s^{-1}) at LB2M and LB3M during autumn 2005, Hurricane Ophelia, and the November event. Positive values denote eastward and onshore currents.

	LB2M		**LB3M**	
Event	along-	across-	along-	across-
Autumn 2005	4.8	1.06	-1.14	3.42
Hurricane Ophelia	7.32	2.93	-2.03	4.6
November Event	7.96	-0.29	4.8	1.5

Significant wave height (H_s) was highly variable over the study period. The occurrence of increased wave height was similar for both sites suggesting that the study area responded to atmospheric forcing (Fig. 7d, e). Site LB2M, however, consistently exhibited lower wave heights than LB3M. Most of the periods of increased wave height were coincident with sustained onshore winds. For example, during the November event, significant wave heights increased, decreased, and then increased again as winds shifted from onshore, to shore parallel, and then back to onshore. The primary exception to this pattern occurred during the passage of Hurricane Ophelia when the strong offshore winds abated and significant wave heights of greater than 1.2 and 1.7 m at LB2M and LB3M, respectively, were observed. Most waves propagated northward and northeastward due to the orientation of the coastline and adjacent shoals. These two directions composed over 96% of the wave field during the study period.

Elevated ABS intensity was usually coincident with increased H_s at both sites. The agreement between ABS and H_s, however, was slightly better at LB2M than at LB3M. When ABS was regressed against H_s, the relationship was weak, but statistically significant. The R^2 values were 0.33 and 0.37 for LB2M and LB3M, respectively, with a $p<0.05$ at both sites. The magnitude of the ABS signal was comparable between the sites except during periods of increased H_s. During these events, the ABS recorded at LB2M exceeded the signal at LB3M despite lower wave heights at LB2M. This pattern may be attributed to the exposure of the underlying fine sand layer at LB2M once the overlying coarse sediments had been mobilized. The underlying sediments at LB2M consisted of 25% mud (compared to <2% mud in the surface sediment at both sites), which was likely resuspended under storm conditions, thus increasing ABS.

Storm-driven Boundary Layer Response to Storms

Event Descriptions: Hurricane Ophelia and November event

Hurricane Ophelia developed from a non-tropical weather system off the east coast of Florida and became the eighth named storm of the 2005 hurricane season at 0600 UTC on 7 September. Over the next seven days, Ophelia's intensity fluctuated with sustained winds between 18 and 38.5 m s^{-1} and strengthened to a category 1 hurricane on four separate occasions during this period (NHC, 2006). At approximately 0000 UTC on 14 September, Ophelia maintained its category 1 status and tracked northeastward parallel to the North Carolina coast over the next two days with maximum winds of 38.5 m s^{-1}. Wind direction was predominantly offshore during but switched to shore parallel on 13 September as the storm passed the study area. The center of circulation never made landfall, but sections of the eyewall passed close to NDBC buoy 41013 in the study area (Fig. 8). Ophelia continued its northward track eventually weakening to a tropical storm at 0000 UTC on 16 September and an extratropical low at 0000 UTC on 18 September (NHC, 2006).

The November event, as described in this paper, refers to the passage of two successive extratropical storm systems that passed through the study area in late November 2005. The first storm system developed from a stationary warm front in the Gulf of Mexico and tracked northeastward toward the study area on 21-22 November. The second storm system originated as a Canadian cold front that converged with another low pressure system east of the Great Lakes on 23-24 November. Using the classification scheme proposed by Dolan and Davis (1992), the event as a whole and the individual storm systems were strong Class 1 storms based on wave height and storm duration. The

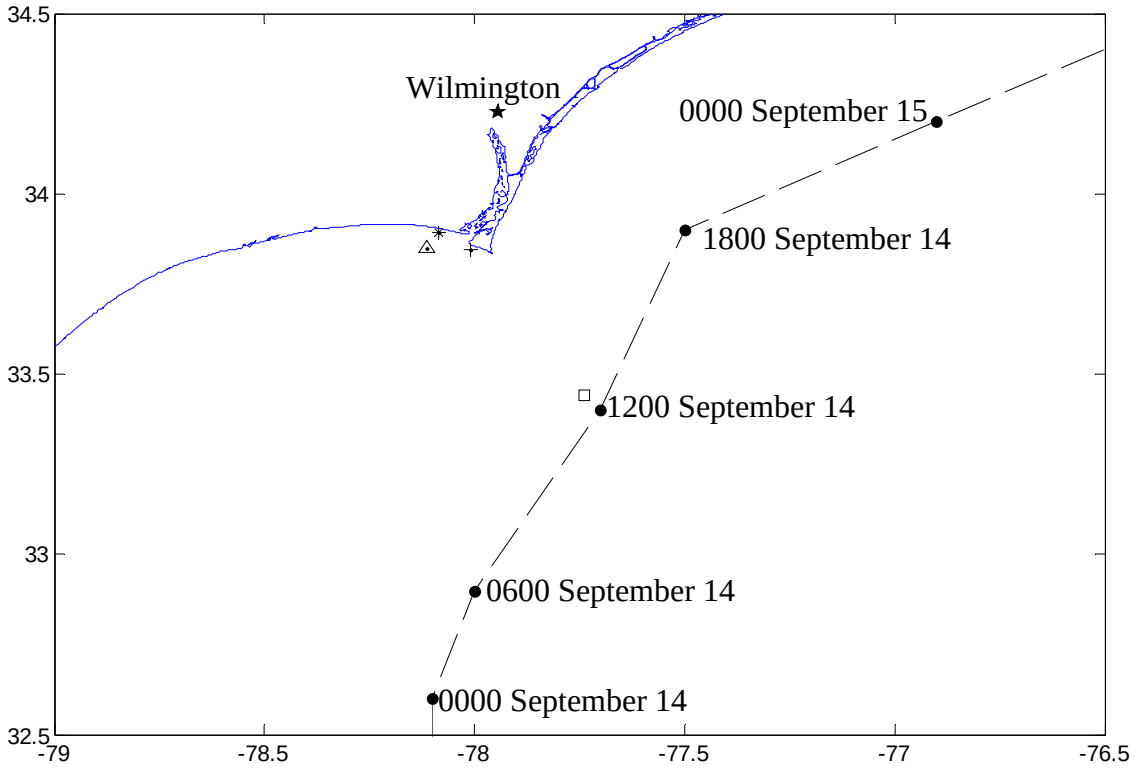

Fig. 8. The track of Hurricane Ophelia through coastal North Carolina from 0000 UTC on 14 September through 0000 UTC on 15 September 2005 (NOAA, 2006). Ophelia remained a category 1 hurricane during its track through coastal North Carolina. Instrumentation is designated by the following symbols: △ = LB1M; * = LB2M; + = LB3M; □ = NDBC buoy 41013.

event's intensity fluctuated with sustained winds between 1.7 and 9.3 m s^{-1} with maximum winds directed onshore (Fig. 7a). The decrease in H_s on 23 November coincided with the brief period (~24 hrs.) between the passage of the two storm systems. The winds shifted again towards onshore, which resulted in maximum H_s as the second storm system impacted the study area on 24 November.

Boundary Layer Response to Meteorological Events at LB2M

Mean near-bottom current magnitude (U_r) was comparable for both of the storm events at LB2M (Fig. 9a, 10a) in spite of large differences in both wind speed and direction between the events. Prior to both events, U_r values were usually less than 10 cm s^{-1} and exhibited a tidal component. As each event impacted the study area, mean bottom currents exceeded the mean pre-storm, fair weather velocity of 10 cm s^{-1}. This increase, presumably of subtidal currents, overwhelmed the tidal component in the time series. During Hurricane Ophelia, bottom currents exceeded 10 cm s^{-1} from 14-18 September and reached a peak of 19.2 cm s^{-1} late on 14 September (Fig. 9a). For the November event, bottom currents exceeded 10 cm s^{-1} for only 1 day (Fig. 10a) and reached a maximum of 20.4 cm s^{-1} on 25 November. For both storms, along-shelf U_r was greater than across-shelf U_r at LB2M.

The velocity of the along-shelf subtidal current exceeded the velocity of the across-shelf current (which was negligible) for both events (Fig. 9b,10b). During Hurricane Ophelia, the along-shelf velocity increased to a maximum of 16 cm s^{-1} toward the east, presumably due to atmospheric forcing by sustained eastward winds. During the November event, the along-shelf velocity was also consistently eastward, reaching a peak of 20.4 cm s^{-1}, which was comparable to the peak velocity during Hurricane Ophelia.

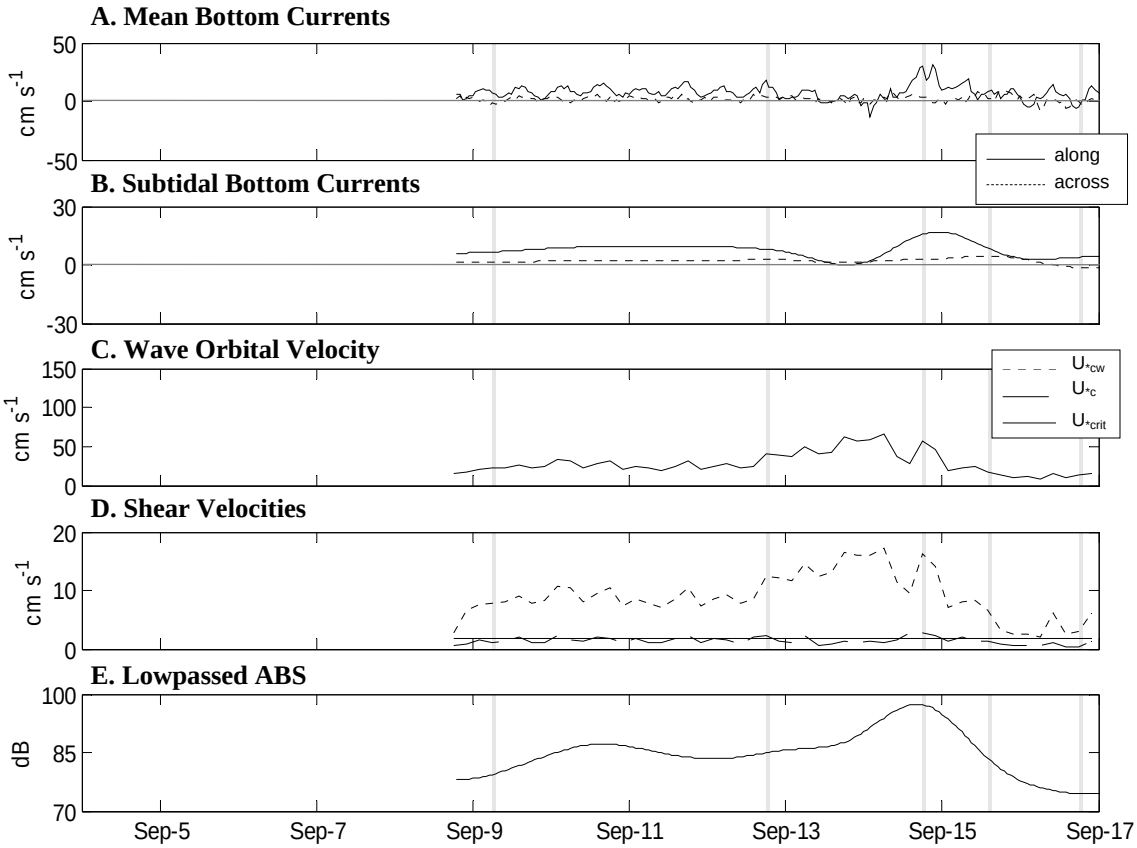

Fig. 9. Bottom boundary layer parameters at LB2M during Hurricane Ophelia. (**a.**) Hourly mean directional bottom currents; (**b.**) Hourly sub-tidal directional bottom currents; (**c.**) Bottom wave orbital velocities; (**d.**) Shear velocities; (**e.**) Lowpassed ABS. Data from 4-8 September are missing due to instrument failure. The positive along-shelf direction is eastward and positive across-shelf direction is onshore. The shadeboxes in the panels represent the bursts used to generate profiles in Fig. 11.

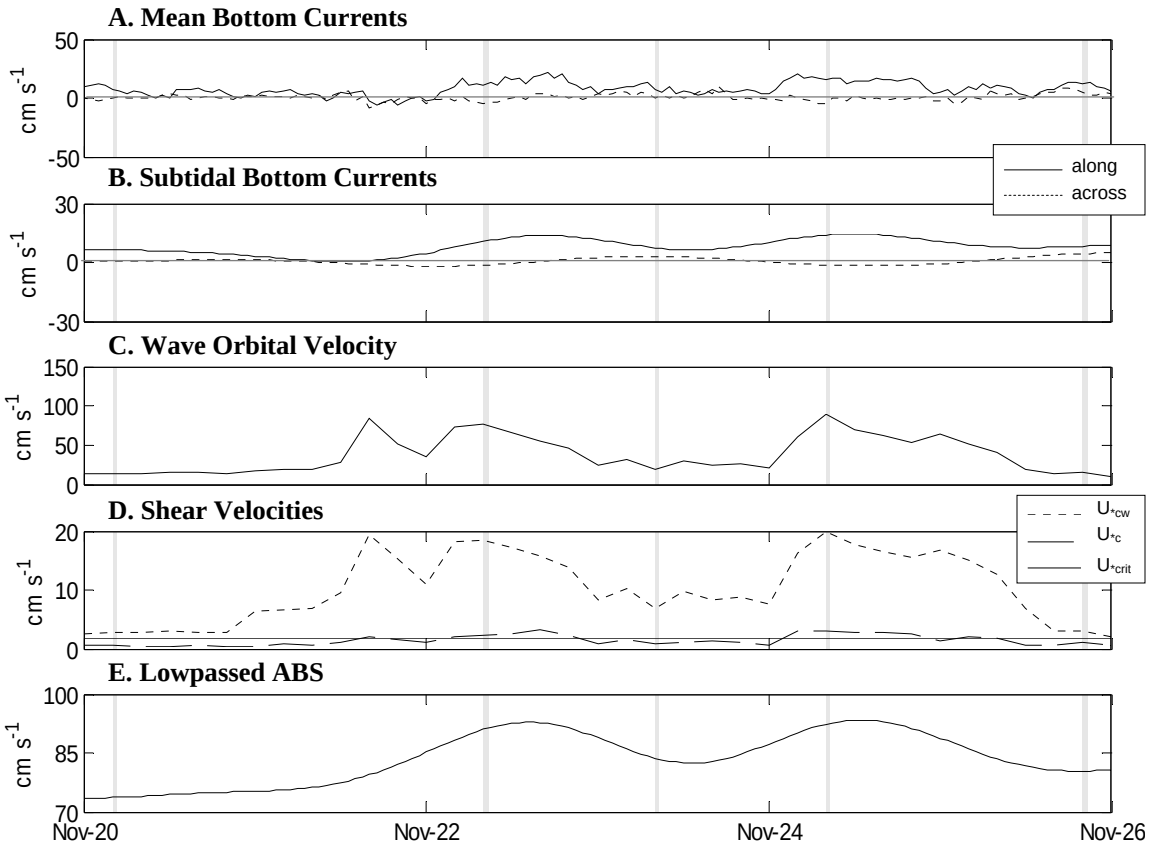

Fig. 10. Bottom boundary layer parameters at LB2M during the November event. (**a.**) Hourly mean along and across-shore bottom currents; (**b.**) Hourly along and across-shore sub-tidal bottom currents; (**c.**) Bottom wave orbital velocities; (**d.**) Shear velocities; (**e.**) Lowpassed ABS. The positive along-shelf direction is eastward and positive across-shelf direction is onshore. The shadeboxes in the panels represent the bursts used to generate profiles in Fig. 12.

One major difference between the two storm events was the duration of elevated subtidal velocities. During the hurricane, elevated subtidal currents (>10 cm s^{-1}) persisted for approximately 1.5 days whereas these currents were elevated for almost 2.5 days during the November event.

Near-bottom wave orbital velocities (U_b) at LB2M showed a similar response to the currents, but the temporal pattern differed between the events. For the hurricane, wave orbital velocities gradually increased during storm approach and then subsided with storm passage. Orbital velocity values in excess of 40 cm s^{-1} were reached about one day prior to the elevation of U_r and the subtidal currents. These U_b values persisted for approximately two days, reaching a maximum of 66.4 cm s^{-1} at 1800 UTC on 14 September 2005 after the eye of the storm had passed to the north of the study area (Fig. 8). For the November event, the temporal variation in wave orbital velocities mirrored changes in U_r and the subtidal currents and peaked at two separate times. As the first storm system approached late on 21 November, U_r , along-shelf subtidal current velocity, and U_b each began to increase although the increase in U_b was initiated about 12 hours before the currents responded. This was most likely due to swell waves impacting the area as first system tracked northward from the Georgia Bight. As the first storm left the study area on 23 November, wind direction rotated clockwise, ultimately reversing direction. This reversal in wind stress at the air-sea boundary opposed the storm-induced water column momentum resulting in the decrease of bottom current and wave orbital velocities to pre-storm levels (Fig. 10b, c). The winds intensified and shifted towards the across-shelf direction on 25 November as the second storm approached resulting in increased current and wave orbital velocities (Fig. 10b) and reaching maximum U_r and U_b

of 20.4 and 89.2 cm s^{-1}, respectively. During both storms, elevated orbital velocities coincided with increased ABS presumably because the energy applied to the seabed increased sediment suspension (Fig. 9e, 10e).

The bbl model output indicated that the velocity necessary to initiate movement of the median grain size, U_{*crit}, was 1.8 cm s^{-1} at LB2M. For both storms, the mean shear velocity due solely to currents, U_{*c}, was approximately 1.4 cm s^{-1} (Fig. 9d, 10d) for most of each event, insufficient to initiate sediment resuspension (Table 2a). Although some of the U_{*c} values exceeded U_{*crit}, they were periodically sustained for a few hours during each event. The shear velocity due to wave-current interaction, U_{*cw}, was between 6 to 9 times greater than U_{*c} for both storms (Table 2a) and exceeded U_{*crit} 100% of the time during both events. Maximum U_{*cw} values were 17.2 cm s^{-1} during Ophelia (1800 UTC 14 September) and 19.9 cm s^{-1} during the November event (0800 UTC 24 November); again well above the value required for sediment movement. As expected, the magnitude of U_{*cw} followed changes in H_s (Fig. 9d, 10d). There was also good agreement between U_{*cw} and along-shelf subtidal current velocity for the November event. Variations in U_{*cw} did not follow subtidal current magnitude during Hurricane Ophelia. Sediment resuspension, as indicated by ABS, closely followed U_b and U_{*cw} for both storms (Figs. 9e, 10e). For the November event, ABS also closely tracked the along-shelf subtidal current velocities (Fig. 10).

Vertical profiles of current velocity, suspended sediment concentration, and sediment transport in the boundary layer also were generated using the bbl model for five sampling bursts throughout each event. Individual bursts were selected that demonstrated the following phases of the storm: pre-storm, increasing currents, peak intensity, waning

Table 2. Summary of the bottom boundary layer response at each site during (a.) Hurricane Ophelia and the (b.) November Event. All parameters are in cm s^{-1}.

A. **LB2M**

	H. Ophelia		November Event	
	Mean	Maximum	Mean	Maximum
U_r	8.4	19.2	9.0	20.4
U_b	29.2	66.4	38.7	89.2
U_{*crit}	1.8	1.8	1.8	1.8
U_{*c}	1.4	2.9	1.3	3.4
U_{*cw}	9	17.2	10.3	19.9

B. **LB3M**

	H. Ophelia		November Event	
	Mean	Maximum	Mean	Maximum
U_r	14.4	71.9	15.3	42.2
U_b	41.9	116.3	63.9	152.2
U_{*crit}	1.3	1.3	1.3	1.3
U_{*c}	1.3	5.1	1.5	3.9
U_{*cw}	6.2	11.9	7.9	14.8

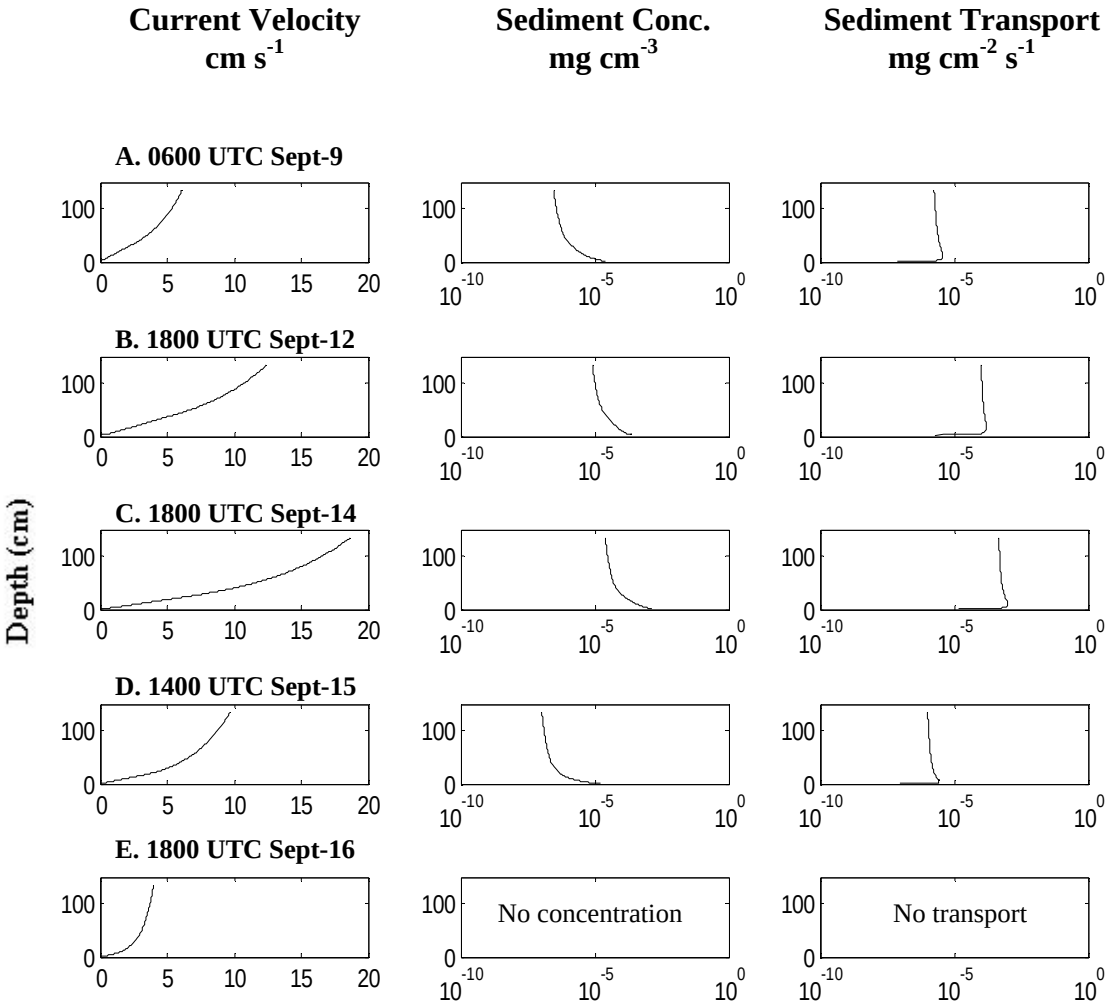

Fig. 11. Bottom boundary layer output for five bursts at LB2M during the passage of Hurricane Ophelia. (**a.**) 0600 UTC 9 September- weak currents; (**b.**) 1800 UTC 12 September- increasing energy; (**c.**) 1800 UTC 14 September- peak storm conditions; (**d.**) 1400 UTC 15 September-waning storm conditions; (**e.**) 1800 UTC 16 September-sediment transport ends. Profile times are denoted as shadeboxes in the time series presented in Fig. 9.

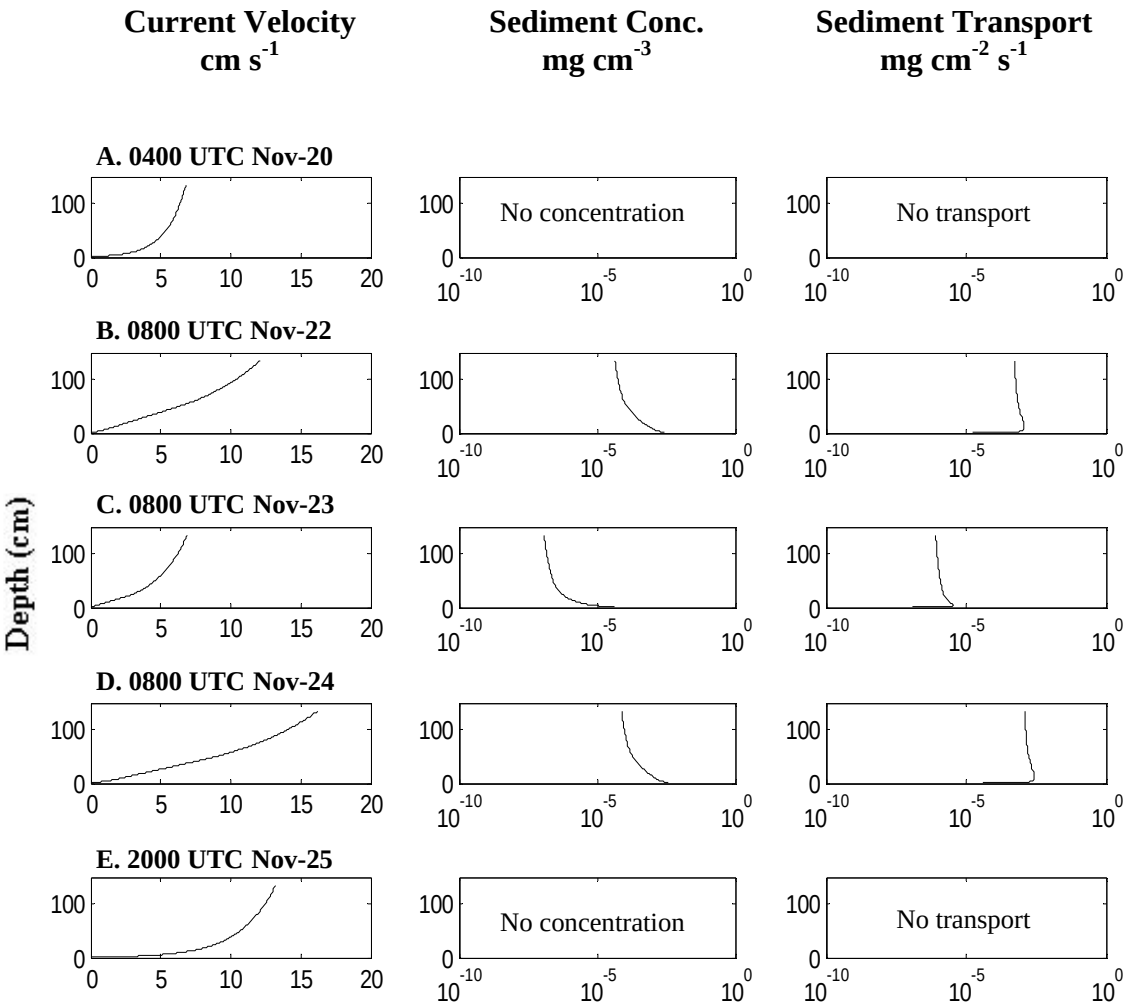

Fig. 12. Bottom boundary layer output at LB2M for five bursts during the passage of the November event. (**a.**) 0400 UTC 20 November- pre-event conditions; (**b.**) 0800 UTC 22 November- passage of first storm; (**c.**) 0800 UTC 23 November- decreasing energy as winds rotated; (**d.**) 0800 UTC 24 November- peak conditions and passage of the second storm; (**e.**) 2000 UTC 25 November- waning storm conditions. Profile times are denoted in the time series presented as shadeboxes in Fig.10.

conditions, and post-storm. Profiles associated with Hurricane Ophelia are shown in Figure 11 and profiles for the November event are shown in Figure 12. Overall, current velocity, suspended sediment concentration, and sediment transport profiles were similar in magnitude for both events at LB2M, but the November event demonstrated similar magnitudes in each of its associated storm systems than Hurricane Ophelia alone.

As Hurricane Ophelia slowly approached the study area from 9-12 September, bottom current velocities were relatively weak within the boundary layer resulting in low suspended sediment concentrations and sediment transport rates within the boundary layer (Fig. 11a). As stronger near-bottom currents and wave orbital velocities emerged on 12 September (Fig. 11b), suspended sediment concentration and transport increased by one and two orders of magnitude, respectively. During peak storm conditions on 14 September (Fig. 11c), suspended sediment concentration and sediment transport increased by yet another order of magnitude presumably in association with the observed increase in boundary layer velocities. Sediment concentration and sediment transport decreased by 2 and 3 orders of magnitude, respectively, by 15 September as boundary layer velocities waned (Fig. 11d). Boundary layer velocities continued to decrease as the storm tracked northeastward, and sediment transport ceased by 1800 UTC on 18 September (Fig. 11d, e).

As the first storm system associated with the November event approached the study area on 20 November, bottom currents were relatively weak within the boundary layer resulting in no sediment transport (Fig. 12a). Boundary layer current velocity began to increase early on 22 November presumably initiating sediment transport in the boundary layer (Fig. 12b). As the first storm system tracked away from the study area,

wind velocity decreased and switched directions on 23 November. Thus concentration and transport in the boundary layer decreased by three orders of magnitude in 24 hours (Fig. 12c). Peak storm conditions were associated with the passage of the second storm system on 24 November as transport increased by three orders of magnitude from the previous day (Fig. 12d). Sediment transport ceased by 2000 UTC on 25 November due to low sediment concentrations within the boundary layer. Based on the bottom boundary layer transport profiles during peak storm conditions, the November event resulted in more transport than Hurricane Ophelia.

Boundary Layer Response to Meteorological Events at LB3M

Mean near-bottom current magnitudes (U_r) were comparable for both events at LB3M, although maximum U_r values during Hurricane Ophelia were almost twice the maximum U_r, observed during the November event. This result differs from LB2M where the maximum U_r for each storm type was of similar magnitude. Prior to the passage of either storm, U_r values rarely exceeded 15 cm s^{-1} (Fig. 13a, 14a) at LB3M. This value contrasts with pre-storm U_r at LB2M, which was approximately 15 cm s^{-1}. As was the case at LB2M, a tidal component was evident in the along-shelf component of the hourly mean bottom current prior to each storm event. However, at LB3M, the tidal component was not lost during storm passage.

For both events, bottom currents increased and ultimately exceeded 15 m s^{-1} the mean pre-storm, fair weather velocity beginning on 14 September and 22 November, respectively (Fig. 13a, 14a). The maximum U_r values at LB3M were 2 to 3.5 times greater than the maximum U_r values at LB2M (Table 2) reaching 72 cm s^{-1} during Hurricane Ophelia and 42 cm s^{-1} during the November event (Fig. 13a, 14a). For both

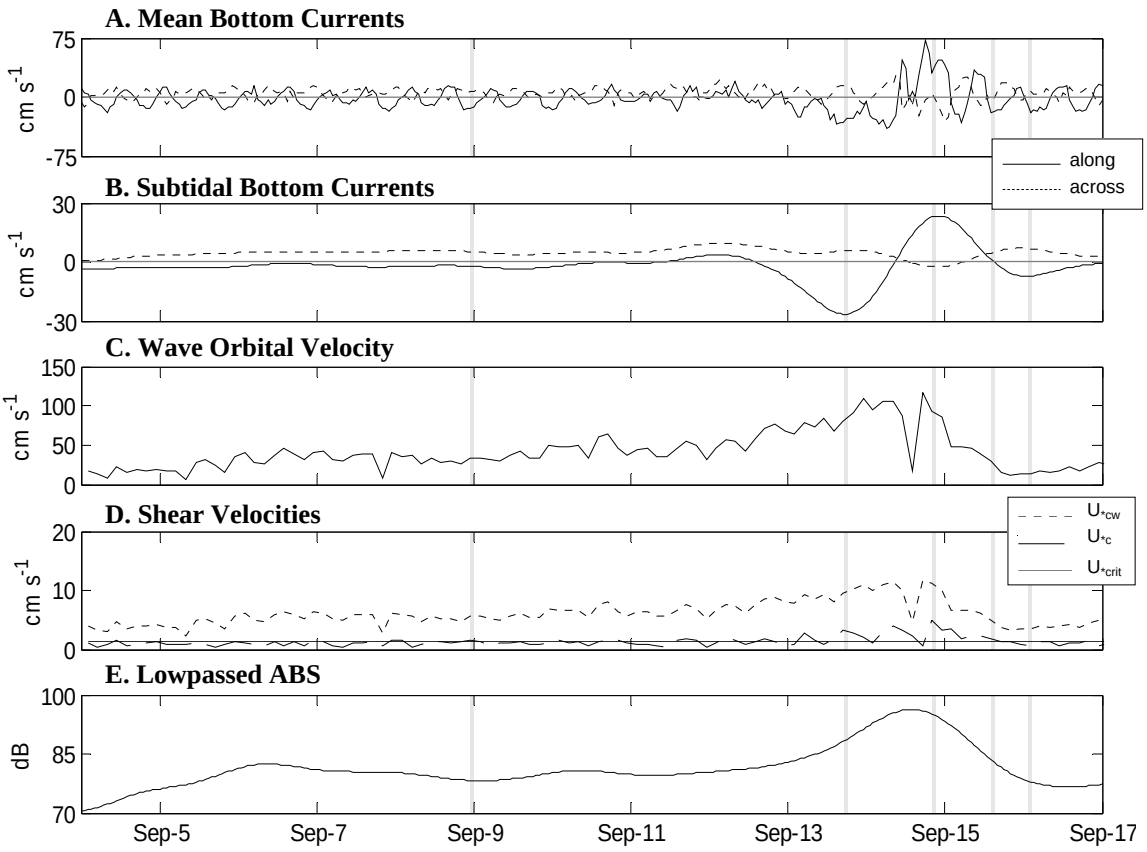

Fig. 13. Bottom boundary layer parameters at LB3M during Hurricane Ophelia. (**a.**) Hourly mean directional bottom currents; (**b.**) Hourly sub-tidal directional bottom currents; (**c.**) Bottom wave orbital velocities; (**d.**) Shear velocities; (**e.**) Lowpassed ABS. The positive along-shelf direction is eastward and positive across-shelf direction is onshore. The shadeboxes in the panels represent the bursts used to generate profiles in Fig. 15.

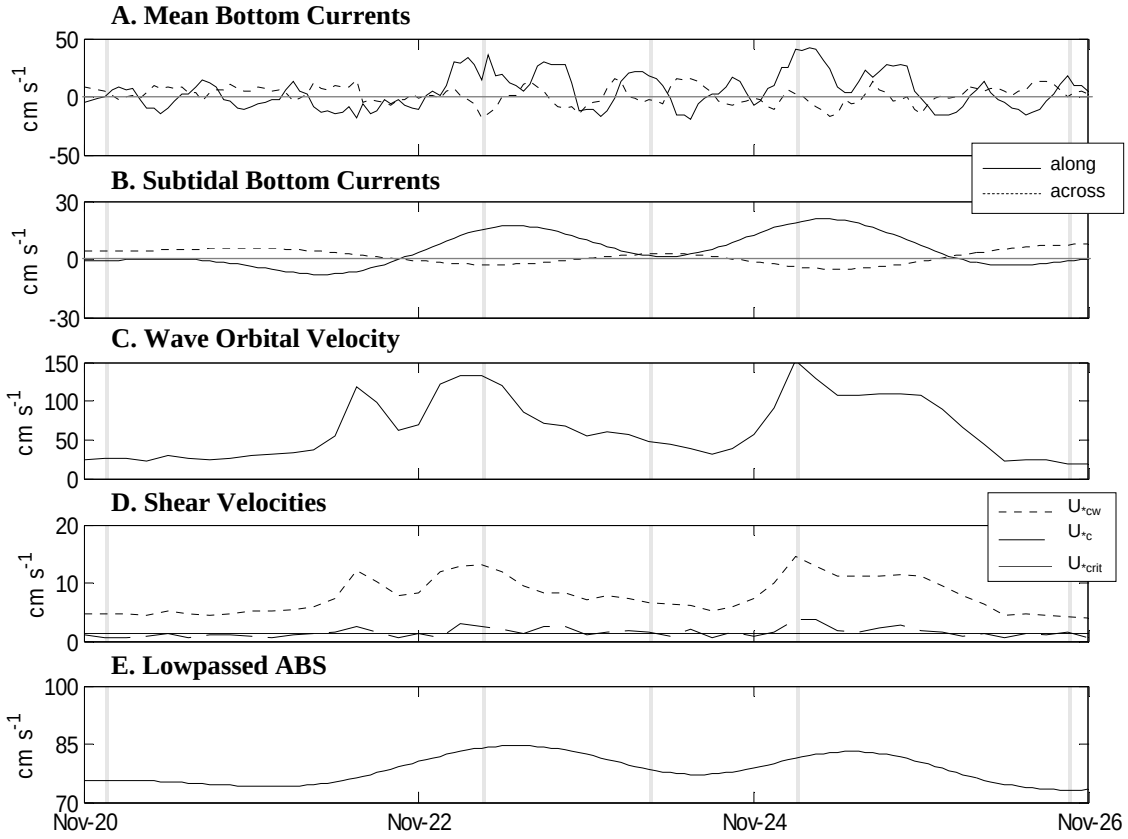

Fig. 14. Bottom boundary layer parameters at LB3M during the November event. (**a.**) Hourly mean directional bottom currents; (**b.**) Hourly sub-tidal directional bottom currents; (**c.**) Bottom wave orbital velocities; (**d.**) Shear velocities; (**e.**) Lowpassed ABS. The positive along-shelf direction is eastward and positive across-shelf direction is onshore. The shadeboxes in the panels represent the bursts used to generate profiles in Fig. 16.

storms, along-shelf U_r was greater than across-shelf U_r, however, unlike LB2M, the difference between along-shelf and across-shelf current magnitude was not as extreme.

As was the case at LB2M, the along-shelf subtidal current magnitude also exceeded the across-shelf current magnitude for both events (Fig. 13b, 14b). During Hurricane Ophelia, the along-shelf subtidal current reversed from westward to eastward due to atmospheric forcing from a shifting wind field (Fig. 7a). This reversal of the along-shelf currents was not observed at LB2M due to a dominant eastward current (Fig. 9b). The maximum velocities in both along-shelf directions at LB3M were approximately 25 cm s^{-1}. A similar reversal was observed in the across-shelf component as the across-shelf currents to move weakly (<2.4 cm s^{-1}) and briefly in the offshore direction (Fig. 13b). During the November event, the along-shelf velocity increased from near zero to 20 cm s^{-1} to the east, which was similar to the peak subtidal current velocity during Hurricane Ophelia. Similar to LB2M, the duration of elevated subtidal currents (>15 m s^{-1}) persisted longer during the November event (3 days) than during Hurricane Ophelia (2.5 days).

Near-bottom wave orbital velocities (U_b) at LB3M showed a similar response to storm passage as the currents (Fig. 13c,14c), but, as observed at LB2M, the temporal pattern differed between the events. Prior to the hurricane, mean U_b values were 35 cm s^{-1} and rarely exceeded 60 cm s^{-1}. As the storm approached, orbital velocity values in excess of 50 cm s^{-1} were reached approximately 1.5 days prior to the elevation of U_r and the subtidal currents. U_b values in excess of 70 cm s^{-1} were sustained for a 2-day period beginning in 13 September. U_b reached a maximum of 116 cm s^{-1} on 14 September (Fig. 13c) after the center of the storm had passed to the north of the study area. The maximum

U_b observed at LB3M during the hurricane was almost two times the magnitude observed at LB2M.

For the November event, the temporal variation in wave orbital velocities mirrored changes in U_r and the subtidal currents and peaked at two separate times. This same pattern was also observed at LB2M. As the first storm system passed through the study area late on 21 November, U_r , along-shelf subtidal current velocity, and U_b each began to increase although the increase in U_b was initiated about 12 hours before the currents responded. Similar to LB2M, this was due to swell waves entering the study area from the south. Pre-storm mean U_b values on the order of 30 cm s^{-1} (Fig. 14b) increased to values in excess of 70 cm s^{-1} on 21 November. These elevated orbital velocities were sustained for 24 hours or about half of the duration of maximum U_b associated with Hurricane Ophelia. Similar to U_r, U_b also declined for about 24 hours; presumably in response to the lull period between the two storm systems. The passage of the second storm system and its associated onshore winds increased current and wave orbital velocities on 25 November (Fig. 14b, c), which reached maximum values of 40.5 cm s^{-1} and 152.2 cm s^{-1}, respectively. During both events at LB3M, elevated orbital velocities coincided with increased ABS (Fig. 13e, 14e). The same pattern was observed at LB2M, but with slightly lower ABS values at LB3M.

The bbl model output indicated that the velocity necessary to initiate movement of the median grain size, $U_{*crit,}$ was 1.3 cm s^{-1} for LB3M (Fig 14d). The mean shear velocity due solely to currents, U_{*c}, was comparable for both storms (Table 2b). The mean U_{*c} during Ophelia was 1.3 cm s^{-1} and the mean for the November event was 1.5 cm s^{-1}. These values are comparable to the U_{*c} reported for both storms at LB2M. At

LB3M, however, due to stronger currents, the mean U_{*c} values were equal to or in excess of the U_{*crit}. The maximum U_{*c} reached during each storm (Table 2b) was 5.1 cm s^{-1} for Hurricane Ophelia (2000 UTC 14 September) and 3.9 cm s^{-1} for the November event (0600 UTC 24 November). These values exceeded U_{*crit}., but were only sustained for short periods of time. These values also exceeded the maximum U_{*c} reported at LB2M for each storm. The shear velocity due to wave-current interaction, U_{*cw}, was between 4 to 6 times greater than U_{*c} for both storms (Table 2b) and exceeded U_{*crit} 100% of the time during both events (Fig. 14d). Maximum U_{*cw} values were 11.9 cm s^{-1} during Ophelia (1700 UTC 14 September) and 14.8 cm s^{-1} during the November event (0600 UTC 24 November); again well above the critical value required for sediment movement. As observed at LB2M, the magnitude of U_{*cw} followed changes in H_s (Fig. 13d, 14d). There also was good agreement between U_{*cw} and along-shelf subtidal current velocities for both of the storm systems associated with the November event with periods of peak U_{*cw} coinciding with peak eastward currents. Maximum U_{*cw} at LB3M also coincided with the peak eastward subtidal current velocity during Hurricane Ophelia (Fig. 13b, c). Sediment resuspension, as indicated by ABS, closely followed U_b and U_{*cw} for both events (Figs. 13 and 14). Maximum ABS values also coincided with peak eastward along-shelf subtidal velocities for both storms (Fig. 13e, 14e).

The LB3M bblm profiles generated for selected sampling bursts during Hurricane Ophelia and the November event are shown in Figures 15 and 16. Overall, current speed, suspended sediment concentration, and sediment transport profiles were similar in shape, but differed in magnitude between the two events at LB3M.

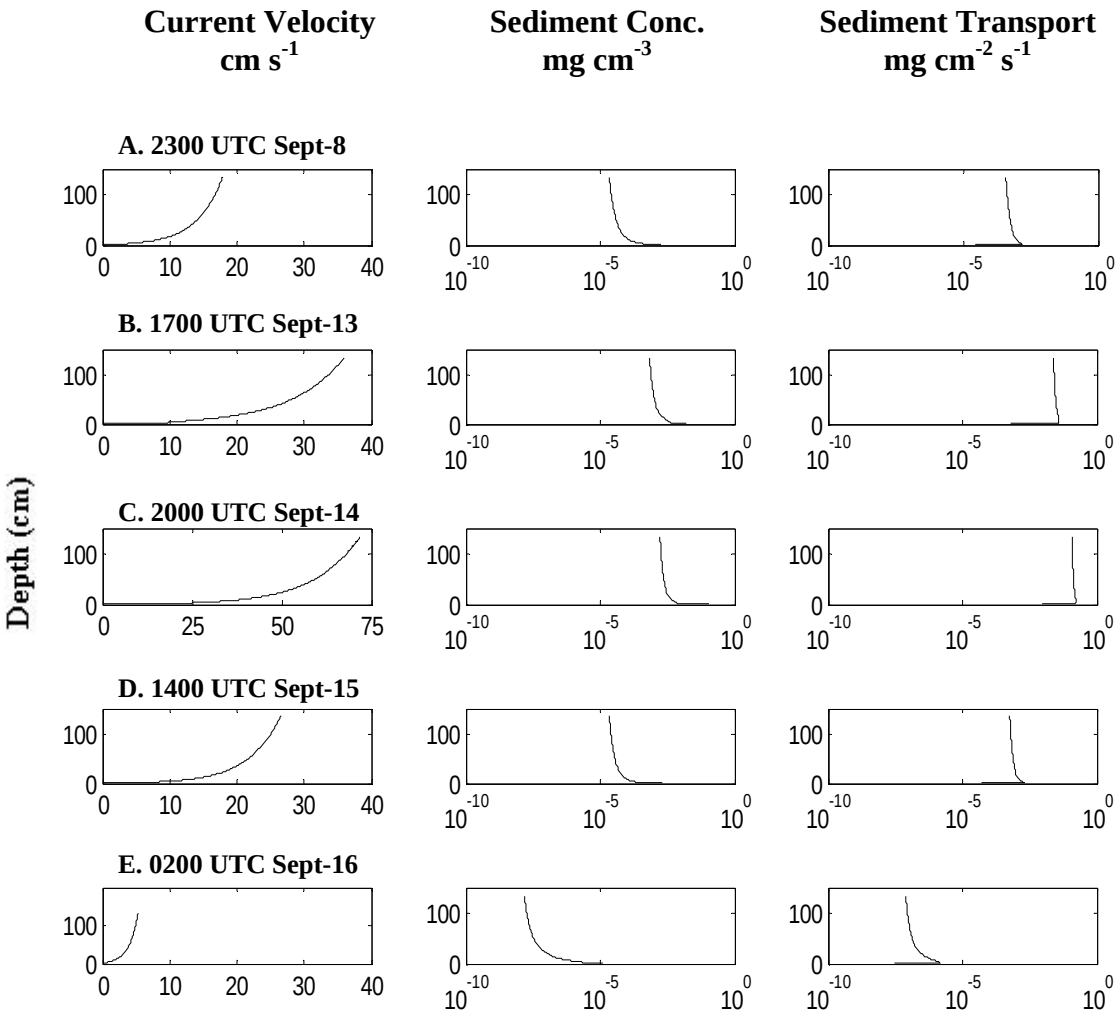

Fig. 15. Bottom boundary layer output for five bursts at LB3M during the passage of Hurricane Ophelia. (**a.**) 2300 UTC 8 September- weak currents; (**b.**) 1700 UTC 13 September- increasing energy; (**c.**) 2000 UTC 14 September- peak storm conditions; (**d.**) 1400 UTC 15 September-waning storm; (**e.**) 0200 UTC 16 September-sediment transport is minimal. The horizontal scale on panel c is higher than the other panels to account for strong currents during Ophelia. Profile times are denoted as shadeboxesin the time series presented in Fig. 13.

Error!

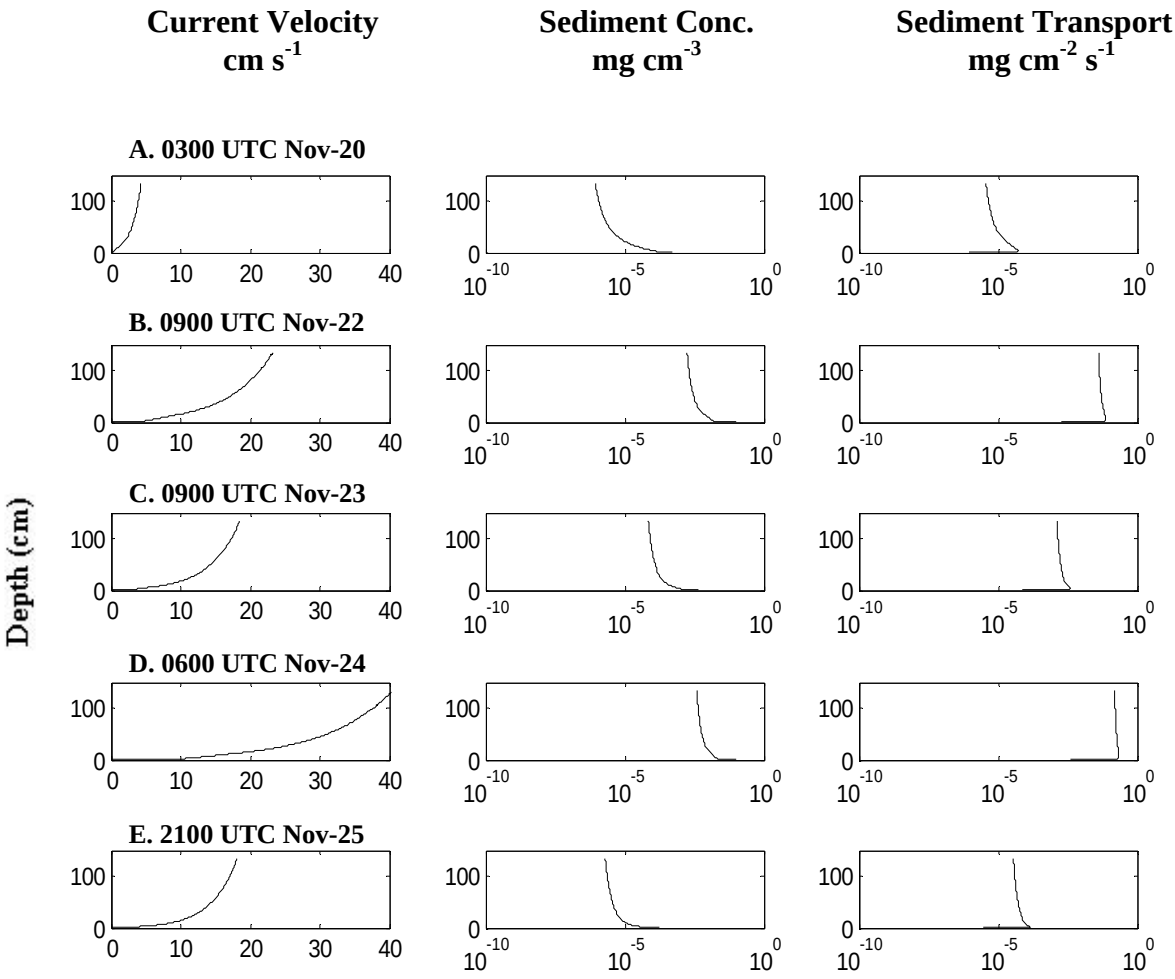

Fig. 16. Bottom boundary layer output for five bursts at LB3M during the passage of the extratropical storm. (**a.**) 0300 UTC 20 November- pre-event conditions; (**b.**) 0900 UTC 22 November- passage of first storm; (**c.**) 0900 UTC 23 November- decreasing energy as winds rotated; (**d.**) 0600 UTC 24 November- peak conditions and passage of the second storm; (**e.**) 2100 UTC 25 November- waning storm conditions. Profile times are denoted as shadeboxes in the time series presented in Fig. 14.

Prior to the passage of Hurricane Ophelia, current velocity and sediment transport rates were minimal (Fig. 15a). As peak storm conditions developed over the study area on 14 September, current velocity increased to 70 cm s^{-1} and sediment transport increased by two orders of magnitude from pre-storm conditions (Fig. 15c). Following Ophelia's passage, current velocity and sediment transport fluxes decreased and both velocities and sediment transport approached pre-storm levels on 15 September (Fig. 15d). Velocities, suspended sediment concentration and sediment transport were negligible by 16 September (Fig. 15d, e).

Similar to LB2M, LB3M exhibited two peaks of high waves and strong currents associated with the passage of two successive storm systems during the November event. These peaks are reflected in the selected bbl model profiles. Prior to the passage of the first storm, weak current velocities and low sediment concentrations resulted in little sediment transport on 20-21 November (Fig. 16a). As the first storm system passed into the study area, current velocity increased to >20 cm s^{-1}, suspended sediment concentrations increased, and sediment transport increased by three orders of magnitude above pre-storm levels (Fig. 16b). Sediment concentration and transport declined on 23 November in association with a period of weak winds and waves between storm systems. By 24 November, current velocities had reintensified in association with the second storm system, exceeding 40 cm s^{-1}, but falling fall short of the maximum velocities associated with Hurricane Ophelia (>70 cm s^{-1}). During peak storm conditions of the November event on 24 November, sediment transport was three times greater than the earlier peak in sediment transport that occurred on 22 November (Fig. 14b, d). Current velocities, suspended sediment concentrations and suspended sediment transport

decreased by 3 orders of magnitude late on 25 November (Fig. 14e) as the storm moved away from the study area.

The bottom boundary layer profiles at LB3M during Hurricane Ophelia exhibited similar spatial and temporal trends as LB2M, but with stronger current velocities, higher sediment concentrations, and elevated sediment transport fluxes. The bottom boundary layer profiles during the November event demonstrated similar spatial and temporal patterns at both sites compared to Hurricane Ophelia. Peak sediment transport fluxes were approximately two orders of magnitude higher at LB3M than LB2M during both events. The November event demonstrated two periods of increased physical forcing in the boundary layer due to passage of two fontal systems during this time contrasted to one period during Hurricane Ophelia. Although the near-bottom mean and subtidal currents associated with the hurricane surpassed those of the November event, the duration of the two periods during the November event was longer. Therefore, the November event should have resulted in higher sediment transport fluxes in the bottom boundary layer than Hurricane Ophelia.

DISCUSSION

Application of the Bottom Boundary Layer Model

As is the case with any physically based quantitative model, the input parameters must reflect natural conditions to accurately predict natural processes. Often, a model is more sensitive to specific parameters thus affecting model output. Such was the case with the bbl model used in this study where mean grain size was used to calculate ripple height, which, in turn, impacted the value of bed roughness (*kb*) and hydraulic roughness

(z_0). The latter was then used to compute the critical shear velocities due to wave-current interaction (U_{*cw}).

One of the parameters generated by the model as it determines *kb* and z_0, is ripple height. When the model was run for LB2M using surficial grain size characteristics, the bbl model predicted ripple heights of approximately 20 cm for both Hurricane Ophelia and the November event. These heights greatly exceeded diver observations at LB2M immediately following the storm. Further, these ripple heights exceeded the total thickness of the coarse sand layer present at the site as recorded in the boxcores (Fig. 17a, 18a). These results called into question the validity of the U_{*cw} values computed for LB2M using the coarse sand as model input.

Slattery (2004) observed variability in sediment texture in the vicinity of LB2M, therefore, other grain size distributions collected within close proximity from our initial sediment samples were gathered from various studies. Ultimately, a new median grain size (0.0268 cm) collected adjacent to LB2M by Battisto and Friedrichs (2002) was used as model input. The revised model output generated by using the revised grain size confirmed the hypothesized effect of grain size in the bottom boundary layer during both events at LB2M (Fig. 17, 18). When using the new grain size, ripple height decreased by about 70% from approximately 20 cm to 5 cm. These ripple heights were more realistic and consistent with diver observations in the study area (Fig. 17a, 18a). U_{*cw} decreased by about 30% during both events due to the change in form drag that resulted from the new grain size input. However, U_{*cw} still exceeded U_{*crit} 100% of the time during both events (Fig. 17b, 18b). The revised shear velocities also were more consistent with the values reported at LB3M and also with values reported from the inner shelf of southern

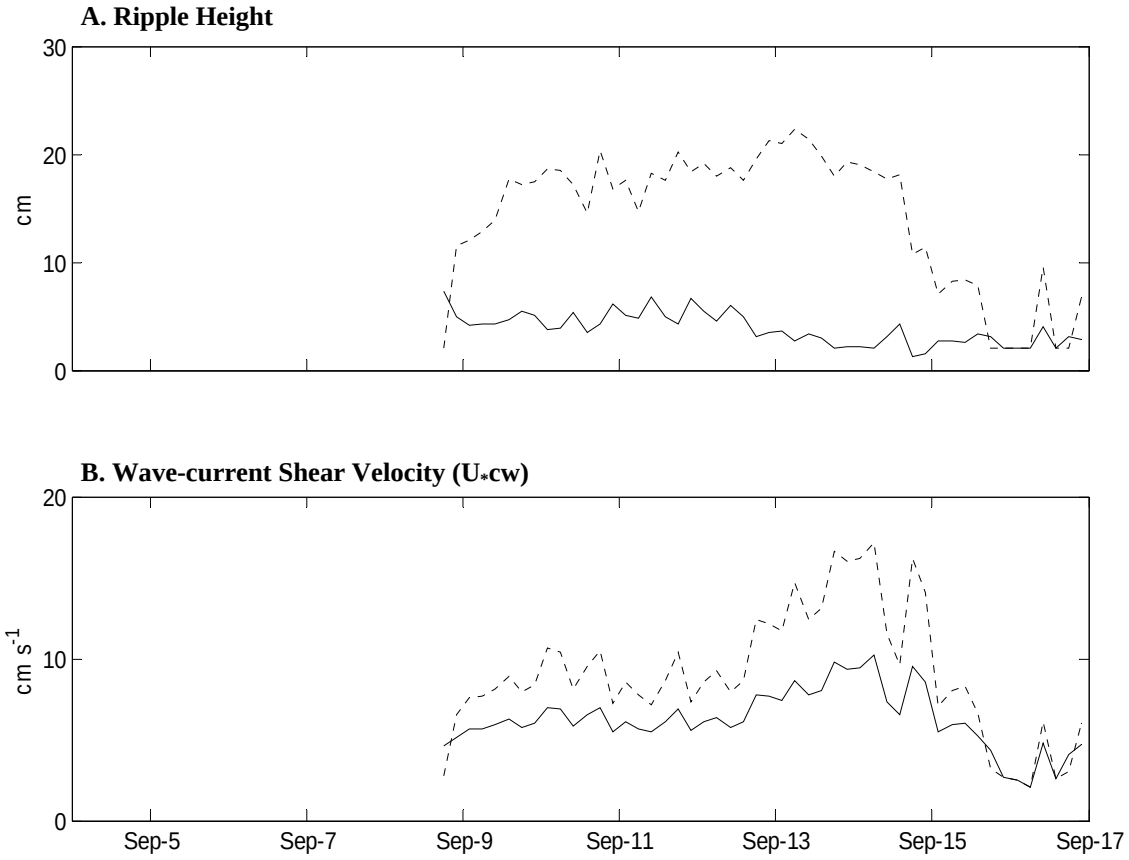

Fig. 17. Comparison of the bottom boundary layer parameters at LB2M during Hurricane Ophelia. (**a.**) predicted ripple height and (**b.**) shear velocity due to wave-current interaction. Dashed lines represent values generated using the original grain size data (0.0645 cm) and solid lines are the revised grain size data (0.0268 cm). Instrument failure occurred from 4-8 September.

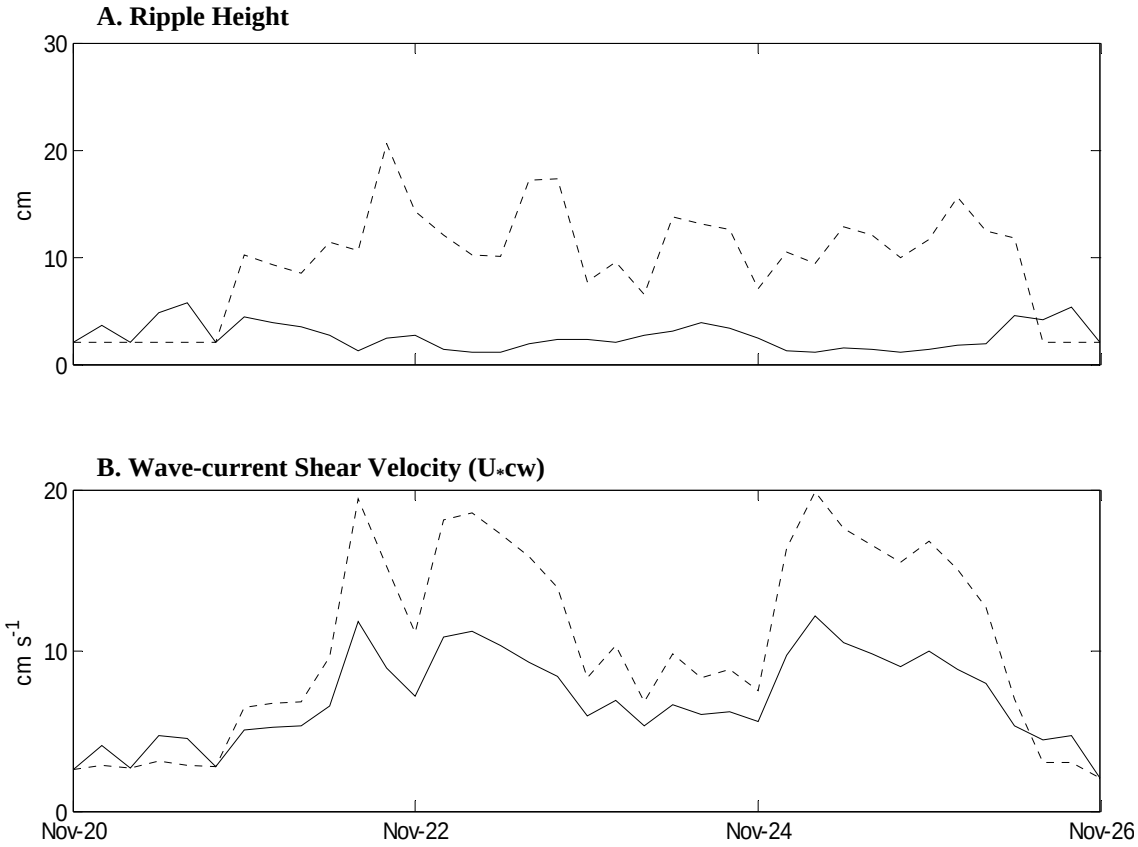

Fig. 18. Comparison of the bottom boundary layer parameters at LB2M during the November event. (**a.**) predicted ripple height (cm) and (**b.**) shear velocity due to wave-current interaction (cm s^{-1}). Dashed lines represent values generated using the original grain size data (0.0645 cm) and solid lines are the revised grain size data (0.0268 cm).

Onslow Bay during Hurricane Isabel (Marshall, 2004). U_{*crit} also decreased from 1.8 to 1.4 cm s^{-1} for the revised grain size input. Consequently, the critical value presumably resulted in more sediment transport within the bottom boundary layer (Fig. 19, 20). Sediment transport fluxes doubled as the result of the revised grain size data at LB2M (Fig. 11, 12, 19, 20). The transport fluxes during each event at LB2M were similar, but two peak fluxes were observed in association with the November event and one peak with Ophelia (Figs. 19, 20). Despite the increase in the transport fluxes at LB2M due to changes in grain size distribution, these fluxes for most bursts remained at least two orders of magnitude lower than the sediment transport fluxes at LB3M during both events (Fig. 15, 16, 19, 20). The depth-integrated fluxes in the bottom boundary layer calculated using the revised grain size data were approximately double the fluxes calculated using the original grain data (Fig. 19, 20). These sediment transport fluxes at peak conditions for each storm demonstrated similar trends. Maximum fluxes occurred at LB3M and were highest during the November event (Table 3, 4). The depth-integrated peak transport fluxes at LB3M during Ophelia and the November event were 17.8 and 23.6 mg cm^{-1} s^{-1}, whereas peak fluxes at LB2M during the events were 0.14 and 0.48 mg cm^{-1} s^{-1}, respectively, again using the revised grain size data. Depth-integrated transport in the boundary layer was approximately two orders of magnitude higher at LB3M than LB2M.

A limitation of the bbl model used in this study is its inability to account for vertical changes in sediment texture that occurred when underlying sediments were exposed at the surface. The wave orbital velocities and strong subtidal currents observed during this study could have easily removed the few centimeters of coarse sand on the

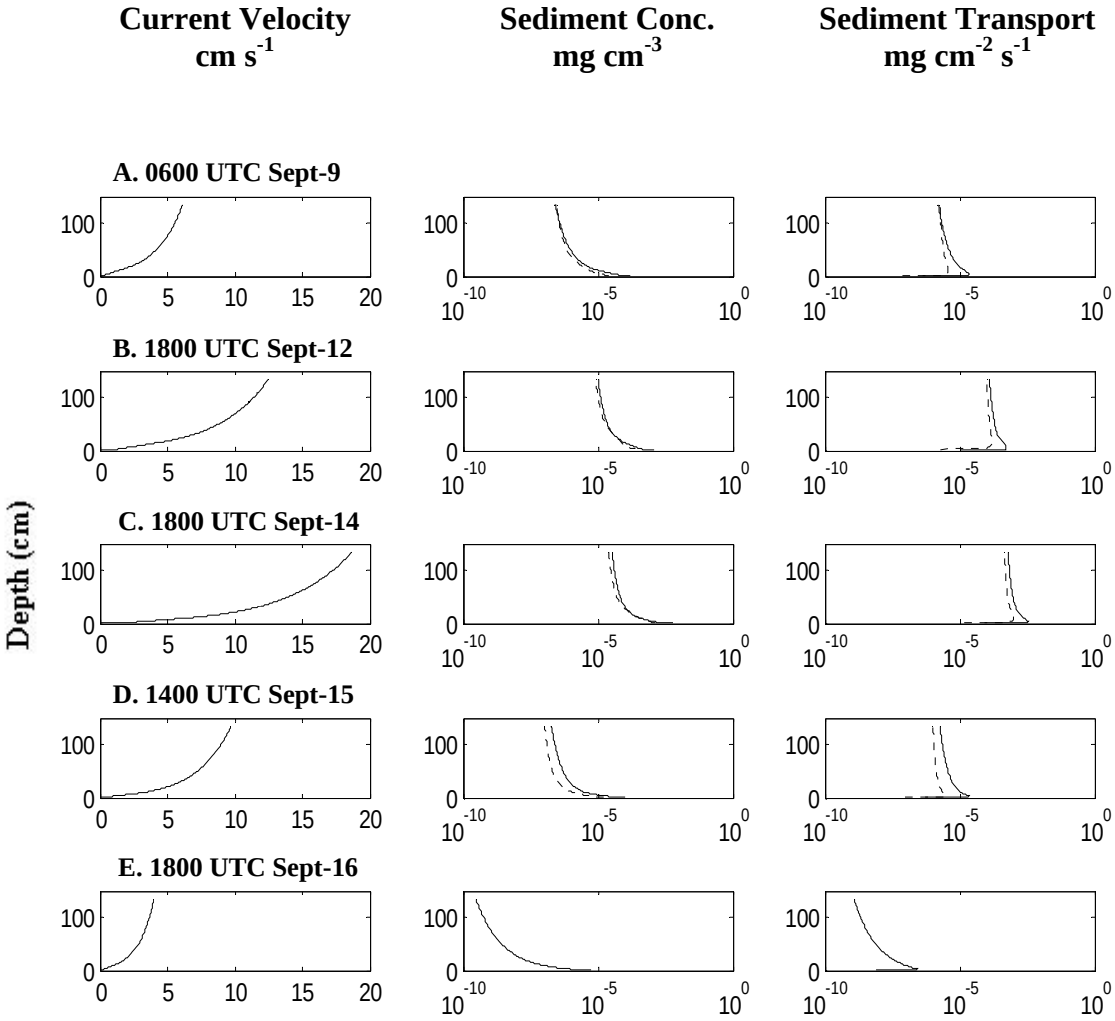

Fig. 19. Bottom boundary layer output for five bursts at LB2M during the passage of Hurricane Ophelia using the original (dashed) and revised (solid) grain size data (**a.**) 0600 UTC 9 September- weak currents; (**b.**) 1800 UTC 12 September- increasing energy; (**c.**) 1800 UTC 14 September- peak storm conditions; (**d.**) 1400 UTC 15 September-waning storm conditions; (**e.**) 1800 UTC 16 September-sediment transport ends. Profile times are denoted in the time series in Fig. 9. No concentration or transport occurred using the original grain size data in panel E.

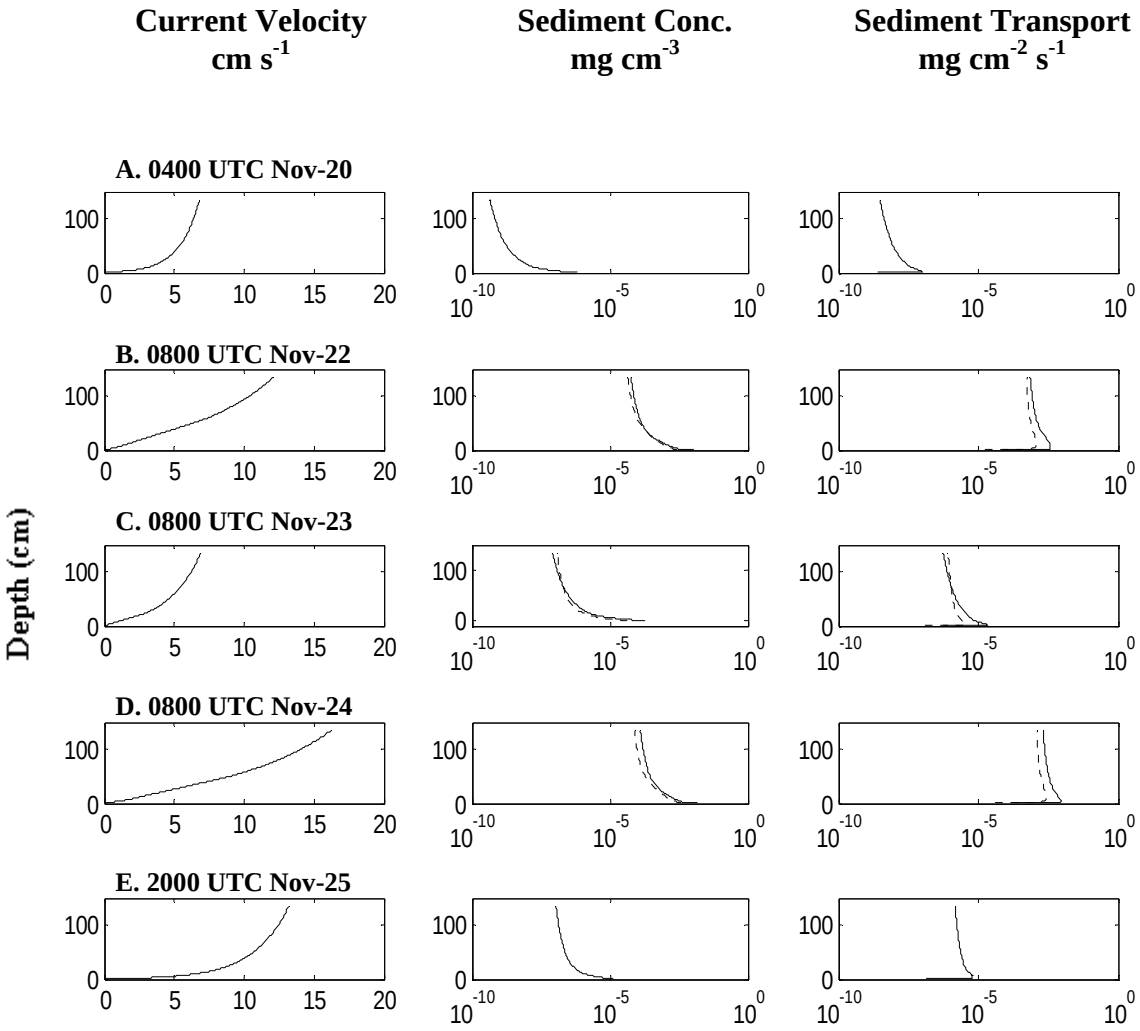

Fig. 20. Bottom boundary layer output for five bursts at LB2M during the passage of the November Event using the original (dashed) and revised (solid) grain size data (**a.**) 0400 UTC 20 November- pre-event conditions; (**b.**) 0800 UTC 22 November- passage of first storm system; (**c.**) 0800 UTC 23 November- decreasing energy in between storms; (**d.**) 0800 UTC 24 November- passage of second storm system and peak conditions; (**e.**) 2000 UTC 25 November- waning physical conditions. Profile times are denoted in the time series in Fig. 9. No concentration or transport occurred using the original grain size data in panels A and E.

Table 3: Depth-integrated sediment transport and associated along-/across-shelf current magnitudes and directions for several bursts during Hurricane Ophelia and the November Event at LB2M.

LB2M							
2005 events	Burst	Burst Time	Depth-integrated sediment transport	Along-shelf currents		Across-shelf currents	
				Magnitude	Direction	Magnitude	Direction
		UTC	(mg cm^{-1} s^{-1})	(cm s^{-1})		(cm s^{-1})	
H. Ophelia	A	0600 Sept-9	6.6×10^{-4}	6.4	east	2.3	onshore
	B	1800 Sept-12	2.9×10^{-2}	7.5	east	3.8	onshore
	C	1800 Sept-14	1.4×10^{-1}	15.8	east	4.8	onshore
	D	1400 Sept-15	5.9×10^{-4}	7.1	east	5.5	onshore
	E	1800 Sept-16	3.0×10^{-6}	4.2	east	0.9	offshore
November Event	A	0400 Nov-20	2×10^{-6}	6.5	east	0.1	offshore
	B	0800 Nov-22	1.8×10^{-1}	10.4	east	2.7	offshore
	C	0800 Nov-23	3.3×10^{-4}	7.8	east	2.1	onshore
	D	0800 Nov-24	4.8×10^{-1}	13.7	east	3.0	offshore
	E	2000 Nov-25	3.3×10^{-4}	8.7	east	3.5	onshore

Table 4: Depth-integrated sediment transport and associated along-/across-shelf current magnitudes and directions for several bursts during Hurricane Ophelia and the November Event at LB3M.

LB3M							
2005 events	Burst	Burst Time (UTC)	Depth-integrated sediment transport (mg cm^{-1} s^{-1})	Along-shelf currents		Across-shelf currents	
				Magnitude ($cm\ s^{-1}$)	Direction	Magnitude ($cm\ s^{-1}$)	Direction
H. Ophelia	A	2300 Sept-8	7.6×10^{-2}	2.0	west	5.5	onshore
	B	1700 Sept-13	3.8×10^{0}	25.9	west	5.6	onshore
	C	2000 Sept-14	1.8×10^{1}	21.0	east	2.0	offshore
	D	1400 Sept-15	1.0×10^{-1}	10.1	east	3.7	onshore
	E	0200 Sept-16	2.7×10^{-5}	7.1	west	6.9	onshore
November Event	A	0300 Nov-20	1.5×10^{-3}	0.6	west	4.2	onshore
	B	0900 Nov-22	6.7×10^{0}	15.3	east	2.7	offshore
	C	0900 Nov-23	2.4×10^{-1}	1.9	east	2.7	onshore
	D	0600 Nov-24	2.4×10^{1}	19.1	east	3.7	offshore
	E	2100 Nov-25	7.2×10^{-3}	1.0	west	7.6	onshore

surface during storm events. Sediment reworking on the scale of 2 to 10 cm has been repeatedly observed during the passage of both hurricanes and extratropical storms over the mid and inner shelf of Onslow Bay (Wren and Leonard 2005). Measurements of sediment thickness collected by divers before and after Hurricane Ophelia at LB1M showed a 10-15 cm increase in sediment thickness, and divers observed a 1 m thick layer of fine suspended material in the vicinity of LB1M 4 days after the same event, which provides evidence for increased sediment mobility during storm events. In a sediment-starved environment, such as Long Bay, such resuspension exposes a variety of underlying materials, which at LB2M, consisted of fine sand. Once exposed on the seabed, the fine sands would undergo significant suspension and transport since the U_{*crit} for these materials is less than the U_{*crit} required to mobilize the overlying coarse material. In much of northern Long Bay, however, the coarse veneer overlies an erosionally resistant substrate (i.e. hardbottom or limestone) (Cleary et al., 2000). If the bbl model was applied to this scenario, the model would significantly over-predict transport.

One valuable modification to the Styles and Glenn (2002) bbl model would be the addition of physical theories and equations that could account for significant changes in grain size over the duration of the time series. If the model accounted for two-dimensional changes in sediment texture, it would provide more realistic transport rates for areas characterized by significant lateral and vertical sediment heterogeneity. Modeling complex interactions of linear and non-linear parameters of the coastal ocean is an arduous task, but the updated bbl model would increase accuracy, thus leading to greater applicability to the modeling of continental shelves.

Influence of Storm Type and Location on Sediment Transport in Long Bay

Numerous studies have documented that sediment transport on the inner shelf is dominated by storm-generated processes (Wright et al., 1986; Wright et al., 1991; Cacchione et al., 1994; Wright et al., 1994; Pepper and Stone, 2002; Wren and Leonard 2005). Bottom stresses resulting from both waves, currents, and their nonlinear interactions initiate sediment mobilization on the inner shelf and influence the amount of sediment that is ultimately available for transport by storm-driven subtidal flows in the along-/across-shelf direction (Trowbridge and Young, 1989; Wright et al., 1991; Wren and Leonard, 2005). While both hurricanes and extratropical storms have demonstrated significant sediment transport on both the mid and inner continental shelf, it has been proposed that extratropical storms may be more significant in terms of overall sediment movement on the inner continental shelf because they occur with greater frequency (Dolan et al., 1988).

To examine the relative impact of site location and storm type on suspended sediment transport in the study area, the along-/across-shelf current magnitudes and directions were compared to the depth-integrated sediment transport fluxes during peak storm conditions in the bottom boundary layer (Fig. 19, 20; Table 3, 4). Because sediment transport was calculated as the product of current velocity and sediment concentration, it was assumed that current direction dictated transport direction. As discussed earlier, along-shelf currents were predominantly eastward, thus suspended sediment transport was eastward as well. These results are consistent with previous studies conducted on the mid and inner continental shelf of Onslow Bay, where the along-shelf component of sediment transport dominated the net transport direction during

both hurricanes and extratropical storms (Marshall, 2004; Wren and Leonard, 2005). These results suggest a potential mechanism for the maintenance of large shoal systems in the study area as the along-shelf currents in Long and Onslow Bays converge toward Cape Fear. The dominant eastward along-shelf currents and transport prevalent during these types of storm systems potentially may transport substantial volumes of sediment to Jay Bird and Frying Pan Shoals, located east of LB2M and LB3M, respectively. Similar to results presented from this region, McNinch and Leuttich (2000) observed converging sediment transport directions on each side of Cape Lookout Shoals during fair weather conditions in northern Onslow Bay.

As with along-shelf transport, the across-shelf transport direction during peak storm conditions was determined by observing the dominant across-shelf current direction. Offshore currents and transport occurred during peak storm conditions in most cases. The only exception was at LB2M during Hurricane Ophelia when weak onshore currents (5 cm s^{-1}) existed during a period of low transport fluxes (0.14 mg cm^{-1} s^{-1}). The net offshore transport documented here for the November event is consistent with the results of Wright et al. (1986) who showed that wind-driven, southerly currents produced by northeaster storms can produce secondary, but strong, downwelling on the inner shelf of the Middle Atlantic Bight.

As proposed by Lyne et al. (1990), Cacchione et al. (1994), and Wren and Leonard (2005), the intensity of bottom stress resulting from the combination of waves and currents also impacted the differences in sediment transport between storm types and between site locations. For the events examined here, depth-integrated peak sediment transport during the November event was approximately 25-70% greater than the depth-

integrated transport for Hurricane Ophelia despite lower subtidal current magnitudes. The H_s, U_b, and U_{*cw}, associated with the November event exceeded U_{*crit} at both sites thereby resulting in resuspension. As long as the subtidal currents were of sufficient strength to maintain the resuspended material in the water column, sediments were transported along-/across-shelf depending on the direction of the prevailing current. Because these currents were sustained in the same direction for longer periods of time during the November event, the net transport for the November event was greater than for the hurricane.

During this study, a class 1 extratropical storm transported more sediment than a category 1 hurricane. Strong hurricanes (e.g. Category 3 and higher) are commonly over-represented in the literature due to their substantial impact on sediment transport and, possibly, to scientists' affinity to study low frequency, catastrophic events. According to historical data from the National Hurricane Center and the Center for Coastal Studies, the frequency of a tropical system, defined as a tropical storm status or greater, impacting the region from 1950-2005 was approximately 0.7 tropical systems per year. If tropical depressions are included, the rate increased to 0.9 per year. Regionally, extratropical storms recur every 3 to 12 days from October through April with approximately 25 storms during this time period (Dolan et al., 1988). Using these data, the frequency of extratropical storms along the North Carolina coast is approximately 30 to 40 times greater than tropical systems. Thus, extratropical storms have a profound importance in determining sedimentological responses due to storms on inner shelf margins over short and long time scales (Wright et al., 1994).

The magnitude of sediment transport also varied between the study sites being approximately two orders of magnitude higher at LB3M than at LB2M. This result is reasonable since LB3M exhibited (1) larger H_s, U_b, and U_{*cw}, (2) stronger subtidal currents, and (3) a smaller mean grain size with a lower U_{*crit} value than site LB2M. Consequently, more sediment was suspended and transported along-/across-shelf at LB3M for the storm events examined in this study. While this study did not attempt to ascertain why the magnitudes of the various physical forcing mechanisms differed between the sites, one potential factor may be their geographical location within Long Bay. LB3M lies in closer proximity to the higher energy shelf of Onslow Bay and, therefore, is less buffered from approaching storms than LB2M. The location of LB3M may have influenced the strong mean bottom currents (>70 cm s^{-1}) observed during Hurricane Ophelia. Local bathymetry and adjacent shoals could have affected approaching waves into the study area as well. LB3M was approximately 1.4 m shallower than LB2M, which could have accounted for the larger wave heights and elevated wave orbital velocity. Depth and U_b exhibit an inverse relationship, so as depth decreases the near-bottom wave orbital velocity increases. Although a number of parameters may have impacted local hydrography and bottom boundary layer dynamics, their effects on sediment transport were not quantified.

Given the high degree of variability in bottom sediments in northern Long Bay and the bbl model's sensitivity to changes in grain size it is difficult to extrapolate the results of this study spatially. Previous work in the study area has shown that the characteristics of bottom samples change both spatially and temporally (Battisto and Friedrichs, 2002; Slattery, 2004). In fact, surface sediment samples collected by divers

for this study showed a complex heterogeneity in sediment texture. For example, at LB2M the samples were collected approximately 200 m apart and exhibited significant variations in grain size. Samples at LB3M were collected about 70 m apart and no discernible variation in grain size was observed. Consequently, it must be assumed that the texture of bottom sediments in this study area may change appreciably over very short distances. The large-scale variability in sediment texture is evident in sidescan sonar mosaics produced for the area (Fig. 21). These images suggest the presence of ripple scour depressions (RSD) filled with coarse-grained sands (light regions) and mud drapes (dark regions). RSDs are common shore-normal features previously identified on the shoreface of Wrightsville Beach, NC in southern Onslow Bay (Thieler et al., 1995, 2001). Diver observations and vibracore surveys have validated the occurrence of both RSD's and extensive mud deposits offshore of northern Long Bay beaches (Cleary et al., 2000).

Implications for Shoreline Sustainability

The beaches shoreward of LB2M and LB3M, Oak Island and Bald Head Island, respectively, undergo frequent renourishment projects to counter the effects of beach erosion (Cleary et al., 2000). However, the rate of beach erosion has maintained pace with renourishment projects, thus transferring large quantities of sediment from the beach onto the shoreface and inner shelf (Pearson and Riggs, 1981). The results of this study suggest that much of the offshore transport occurs during the passage of extratropical storms. Since sea turtle nesting season lasts from May through October, various regulations and guidelines force beach renourishment projects to occur during the early spring to minimize the environmental impact on these endangered and protected species. During this time the frequency of extratropical storms is still relatively high with an

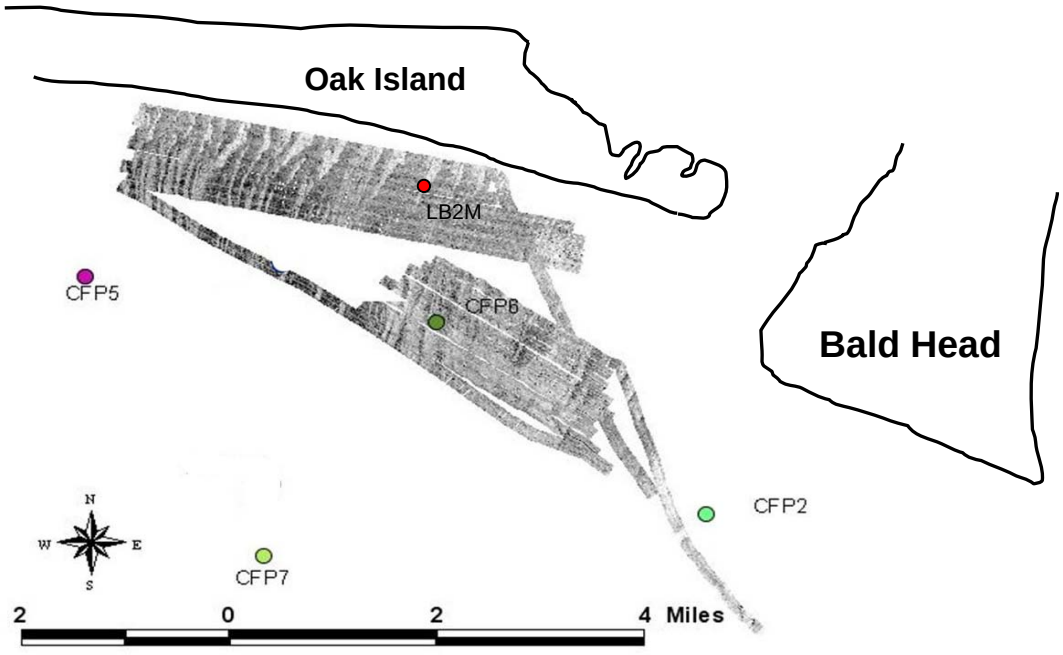

Fig. 21. A sidescan mosaic in the vicinity of LB2M demonstrating variations in grain sized based on relative acoustic backscatterance of the sediment types. The other sites can be ignored for this study.

average of 4 storms each month (Dolan et al., 1988). These storms could potentially cause increased wave energy on the beach, thus eroding the newly placed renourishment sand onto the nearshore. Quantifying the magnitude and direction of sediment transport events during different types of storms would improve our understanding of their associated sedimentological responses in the nearshore environment. After monitoring storm-driven sediment transport over a long period and incorporating historical storm data, a statistical analysis could be performed to assist public officials in determining the optimal timing for beach renourishment to occur in relation to storm frequency and magnitude, thus maximizing the overall success of these costly public projects.

CONCLUSIONS

The hydrography and bottom boundary layer dynamics during the autumn of 2005 were characterized by the passage of Hurricane Ophelia and several low magnitude extratropical events. These events produced similar trends in wave height, mean and subtidal current velocities, wind speed, ABS during the autumn of 2005 at both sites. The inability of the bbl model to account for significant variations in lateral and vertical sediment heterogeneity resulted in the use of a revised grain size distribution as model input than collected during this study. The magnitude at which the sites responded to storm-driven physical forcing mechanisms demonstrated some variation. Wave height and current velocities at LB3M exhibited higher magnitudes than LB2M during both events. This elevated amount of wave-current interaction in the boundary layer coupled with substantial subtidal current velocities and smaller grain size distribution resulted in two orders of magnitude higher in sediment transport at LB3M. Bottom boundary layer sediment transport was several orders of magnitude higher during events than during fair

weather conditions and was 25-70% higher during the November event due to increased wave height than during Hurricane Ophelia. Sediment transport was dominated by the along-shelf component, which was consistent with current direction.

REFERENCES

Atkinson, L.P., Menzel, D.W., 1985. Introduction: Oceanography of the Southeastern U.S. Continental Shelf. In: Atkinson, L.P., Menzel, D.W., Bush, K.A. (Eds.), Oceanography of the Southeastern U.S. Continental Shelf. American Geophysical Union, Washington, D.C., pp. 1-9.

Battisto, G.A., 2000. Field measurement of mixed grain size suspension in the nearshore under waves. Ph.D. Thesis, Virginia Institute of Marine Science, Gloucester Point, VA, unpublished.

Battisto, G.M., Freidrichs, C.T., 2002. Sediment Entrainment Devices Mound Study 6000-21 Cape Fear, NC July-September 2001, Virginia Institute of Marine Sciences, Gloucester Point, VA.

Blanton, J.O., Schwing, F.B., Weber, A.H., Pietrafesa, L.J., Hayes, D.W. 1985. Wind Stress Climatology in the South Atlantic Bight. In: Atkinson, L.P., Menzel D.W., Bush, K.A. (Eds.), Oceanography of the Southeastern U.S. Continental Shelf., American Geophysical Union, Washington, D.C., pp. 10-22.

Cacchione, D.A., Drake, D.E., Ferreira, J.T., Tate, G.B., 1994. Bottom stress estimates and sand transport on northern California inner continental shelf. Continental Shelf Research, 14(10-11): 1273-1289.

Carpenter, J.H. and Yonts, W.L., 1979. Freshwater Inflow to the Cape Fear River Estuary, NC October 1951-September 1979 (Appendix A), Carolina Power and Light Company, Raleigh, NC.

Cleary, W.J., McLeod, M.A., Rauscher, M.A., Johnston, M.K., Riggs, S.R., 2000. Beach Renourishment on Hurricane Impacted Barriers in Southeastern North Carolina, USA: Targeting Shoreface and Tidal Inlet Sand Resources. Journal of Coastal Research- Special Issue, 34: 232-255.

Deines, K.L., 1999. Backscatter estimation using broadband acoustic doppler current profilers. Oceans ’99 MTS/IEEE Conference Proceedings, 13-16.

Dolan, R., Davis, R.E., 1992. Rating Northeasters. Mariners Weather Log, 36: 4-16.

Dolan, R., Lins, H., Hayden, B., 1988. Mid-Atlantic coastal storms. Journal of Coastal Research, 4: 417-433.

Folk, R.L., 1980. Petrology of Sedimentary Rocks: Hemphill Publishing Co., Austin, Texas, 184 pp.

Glenn, S.M., Grant, W.D., 1987. A suspended sediment correction for combined wave and current flows. Journal of Geophysical Research, 92 (C8): 8244-8264.

Grant, W.D., Madsen, O.S., 1979. Combined wave and current Interaction with a rough bottom. Journal of Geophysical Research, 84 (C4): 1797-1808.

Hoffman, C.W., Grosz, A.E. , Nickerson, J.G., 1999. Stratigraphic framework and heavy minerals of the continental shelf of Onslow and Long bays, North Carolina. Marine Georesources and Geotechnology, 17: 173-184.

Hupp, C.R., 2000. Hydrology, geomorphology, and vegetation of Coastal Plain rivers in the southeastern USA. Hydrological Processes, 14: 2991-3010.

Kim, S.-C., Wright, L.D., Kim, B.-O., 1997. The combined effects of synoptic-scale and local scale meterological events on bed stress and sediment transport on the inner shelf of the Middle Atlantic Bight. Continental Shelf Research, 17 (4): 407-433.

Lyne, V.D., Butman, B., Grant, W.D., 1990. Sediment movement along the U.S. east coast continental shelf- I. Estimates of bottom stress using the Grant-Madsen model and near-bottom wave and current measurements. Continental Shelf Research, 10(5): 397-428.

Madsen, O.S., Wright, L.D., Boon, J.D., Chisholm, T.A., 1993. Wind stress, bed roughness and sediment transport on the inner shelf during an extreme storm event. Continental Shelf Research, 13 (11): 1303-1324.

Mallin, M.A., 2006. The Ecology of the Cape Fear River System. http://www.uncwil.edu/riverrun/river_tutorial/CFRSystem.htm.

Marshall, J.A., 2004. Event driven sediment mobility on the inner continental shelf of Onslow Bay, NC. Master's Thesis, University of North Carolina Wilmington, Wilmington, NC, unpublished.

McLeod, M.A., Cleary, W.J., 2000. Beach replenishment for hurricane impacted Oak Island, NC; targeting shoreface sand resources. Abstracts with Programs: Geological Society of America Annual Meeting, 32 (2): 61.

McNinch, J.E. Luettich, Jr. R.A., 2000. Physical processes around a cuspate foreland headland: implications to the evolution and long-term maintenance of a cape-associated shoal. Continental Shelf Research, 20 (17), 2367-2389.

National Hurricane Center, 2006. 2005 Atlantic Hurricane Season- Hurricane Ophelia. http://www.nhc.noaa.gov/pdf/TCR-AL162005_Ophelia.pdf.

National Oceanic and Atmospheric Administration, 2006. Tide Tables: North Carolina-South Carolina. http://tidesandcurrents.noaa.gov/tides04/tab2ec3a.html.

Pawlowicz, R., Beardsley, B., Lentz, S., 2002. Classical tidal harmonic analysis including error estimates in MATLAB using T TIDE. Computer & Geosciences, 28: 929-937.

Pearson, D.R., Riggs, S.R., 1981. Relationship of surface sediments on the lower forebeach and nearshore shelf to beach nourishment at Wrightsville Beach, North Carolina. Shore and Beach, 49: 26-31.

Pepper, D.A. and Stone, G.W., 2002. Atmospheric forcing of fine-sand transport on a low-energy inner shelf: south-central Louisiana, USA. Geo-Marine Letters, 22: 33-41.

Pietrafesa, L.J., Janowitz, G.S., Wittman, P.A., 1985. Physical oceanographic processes in the Carolina Capes Physical oceanographic processes in the Carolina Capes. Atkinson, L.P., Menzel, D.W., Bush, K.A. (Eds.), Oceanography of the Southeastern U.S. Continental Shelf. American Geophysical Union, Washington, D.C., pp. 23-32.

Renfro, A.A., Leonard, L.A., Croft, A.L., 2004. Sediment transport and deposition in tidal riparian wetlands during drought conditions. Eos Trans. American Geophysical Union, 85 (47), Fall Meet. Suppl., Abstract H41C-0305.

Slattery, M.P., 2004. The Influence of the Cape Fear River on Characteristics of shelf sediments in Long Bay, North Carolina. Master's Thesis, University of North Carolina Wilmington, Wilmington, NC, unpublished.

Styles, R., Glenn, S.M., 2000. Modeling stratified wave and current bottom boundary layers on the continental shelf. Journal of Geophysical Research, 105(C10): 24,119-24,139.

Styles, R., Glenn, S.M., 2002. Modeling bottom roughness in the prescence of wave-generated ripples. Journal of Geophysical Research, 107: 1-15.

Thieler, E.R., Brill, A.L., Cleary, W.J., Hobbs, C.H., Gammisch, R.A., 1995, Geology of the Wrightsville Beach shoreface: Implications for the concept of shoreface profile of equilibrium. Marine Geology, 126: 271-287.

Thieler, E.R., Pilkey, O.H., Cleary, W.J., Schwab, W.C., 2001. Modern sedimentation on the shoreface and inner continental shelf at Wrightsville Beach, North Carolina, U.S.A. Journal of Sedimentary Research, 71(6): 958-970.

Traykovski, P., Hay, A., Irish, J.D., Lynch, J.F., 1999. Geometry, migration, and evolution of wave orbital ripples at LEO-15. Journal of Geophysical Research, 104: 1505-1524.

Trowbridge, J., Young, D., 1989. Sand transport by unbroken water waves under sheet flow conditions. Journal of Geophysical Research, 94(C8): 10971-10991.

Williams, J.J., Rose, C.P., 2001. Measured and predicted rates of sediment transport in storm conditions. Marine Geology, 179: 121-133.

Wren, P.A., 2004. Sediment transport measurements on the mid-continental shelf in Onslow Bay, North Carolina. Ph.D. Thesis, North Carolina State University, Raleigh, unpublished.

Wren, P.A. and Leonard, L.A., 2005. Sediment transport on the mid-continental shelf in Onslow Bay, North Carolina during Hurricane Isabel. Estuarine, Coastal and Shelf Science, 63: 43-56.

Wright, L.D., Boon, J.D., III, Green, M.O., List, J.H., 1986. Response of the midshoreface of the southern Mid Atlantic Bight to a "Northeaster". Geo-Marine Letters, 6: 153-160.

Wright, L.D., Boon, J.D., Kim, S.C. and List, J.H., 1991. Modes of cross-shore sediment transport on the shoreface of the Middle Atlantic Bight. Marine Geology, 96: 19-51.

Wright, L.D., Xu, J.P., Madsen, O.S., 1994. Across-shelf benthic transports on the inner shelf of the Middle Atlantic Bight during the “Halloween Storm” of 1991. Marine Geology, 118: 61-77.

Xu, J.P., Wright, L.D., 1998. Observations of wind generated currents of Duck, North Carolina. Journal of Coastal Research, 14: 610-619.

BIOGRAPHICAL SKETCH

Luke Davis was born in Savannah, Georgia on June 26, 1981. He graduated Magna Cum Laude from Georgia Southern University in 2004 with a Bachelor of Science in Geology and a minor in Geography. Luke was a geology tutor and research assistant while completing his undergraduate degree. He participated in the W.M. Keck Geology Consortium at Carleton College (MN) in 2001 and the River Basins Research Initiative at Furman University (SC) in 2003. His undergraduate thesis was entitled, “An investigation of joint sets and their relation to occurrences of rare biota at the Broxton Rocks Preserve, Altamaha Formation (Miocene), Coffee County, Georgia." He participated in other research projects that included hydrogeology, aqueous geochemistry, and planetary geology. In August 2004, he entered the graduate program at the University of North Carolina Wilmington where he worked under the guidance of Dr. Lynn Leonard as a component of the Coastal Ocean and Research Monitoring Program (CORMP) funded through NOAA. Preliminary research from this project was presented at the 2006 Ocean Sciences Meeting in Honolulu, HI in February 2006. Luke is a member of the American Institute of Professional Geologists (AIPG), American Geophysical Union (AGU), Geological Society of America (GSA), and Sigma Xi. Mr. Davis has been published in *Southeastern Geology* in 2005 along with several abstracts for various conferences. He aspires to continue his academic pursuits by conducting academic research, attending professional meetings, and submitting manuscripts for publication.